ISTANBUL TECHNICAL UNIVERSITY ★ GRADUATE SCHOOL

ADDRESSING PARAMETRIC UNCERTAINTIES IN AUTONOMOUS CARGO SHIP HEADING CONTROL

M.Sc. THESIS

Ahmad Irham JAMBAK

Mechatronics Engineering Department

Mechatronics Engineering Programme

JULY 2023

ISTANBUL TECHNICAL UNIVERSITY ★ GRADUATE SCHOOL

ADDRESSING PARAMETRIC UNCERTAINTIES IN AUTONOMOUS CARGO SHIP HEADING CONTROL

M.Sc. THESIS

Ahmad Irham JAMBAK
(518211022)

Mechatronics Engineering Department

Mechatronics Engineering Programme

Thesis Advisor: Asst. Prof. Dr. İsmail BAYEZİT

JULY 2023

İSTANBUL TEKNİK ÜNİVERSİTESİ ★ LİSANSÜSTÜ EĞİTİM ENSTİTÜSÜ

OTONOM KARGO GEMİSİ YÖN KONTROLÜNDEKİ PARAMETRİK BELİRSİZLİKLERİN ELE ALINMASI

YüKSEK LİSANS TEZİ

Ahmad Irham JAMBAK
(518211022)

Mekatronik Mühendisliği Anabilim Dalı

Mekatronik Mühendisliği Programı

Tez Danışmanı: Asst. Prof. Dr. İsmail BAYEZİT

TEMMUZ 2023

Ahmad Irham JAMBAK, a M.Sc. student of ITU Graduate School student ID 518211022, successfully defended the thesis entitled "ADDRESSING PARAMETRIC UNCERTAINTIES IN AUTONOMOUS CARGO SHIP HEADING CONTROL ", which he/she prepared after fulfilling the requirements specified in the associated legislations, before the jury whose signatures are below.

Thesis Advisor :	**Asst. Prof. Dr. İsmail BAYEZİT** Istanbul Technical University	.....
Jury Members :	**Asst. Prof. Dr. İsmail BAYEZİT** Istanbul Technical University	.....
	Prof. Dr. Ömer Kemal KINACI Istanbul Technical University	.....
	Assoc. Prof. Dr. Ferdi ÇAKICI Yıldız Technical University	.....

Date of Submission : 10 July 2023
Date of Defense : 13 July 2023

To my family,

FOREWORD

In the name of Allah, the Most Gracious, the Most Merciful.

Writing a thesis marks a significant milestone in one's academic journey—a culmination of years of dedication, perseverance, and the pursuit of knowledge. As I stand at the threshold of completing this transformative endeavor, I am filled with gratitude and humility for the invaluable support and guidance I have received along the way.

First and foremost, I would like to express my deepest appreciation to my advisor, Asst. Prof. Dr. İsmail Bayezit, for his exceptional mentorship throughout this academic journey. His insightful suggestions, unwavering encouragement, and invaluable expertise have been instrumental in shaping the trajectory of my work. His dedication to fostering a stimulating academic environment and his commitment to my intellectual growth have truly been a source of inspiration.

I would also like to extend my heartfelt gratitude to my parents, Muhammad Irfan Jambak and Nurhasanah Wuri Utami, for their unwavering love, encouragement, and unwavering support throughout my life and academic pursuits. Their belief in my abilities and their constant encouragement have been a guiding light, providing me with the strength and motivation to overcome challenges and pursue excellence.

Furthermore, I am grateful for the camaraderie and collaboration I have experienced with my lab colleagues from the Model-Based Design Lab. The stimulating discussions, shared insights, and mutual support have created a vibrant and enriching research environment. I am indebted to each and every one of them for their intellectual contributions, friendship, and the sense of belonging they have fostered within our lab.

I would also like to express my gratitude to Türkiye Bursları for awarding me the scholarship that has made my academic journey possible. Their generous support has not only provided me with financial assistance but has also opened doors to new opportunities, allowing me to pursue my studies in a diverse and enriching environment.

Finally, I would like to express my gratitude to all the teachers, professors, and mentors who have influenced my academic journey and shaped my intellectual growth. Their knowledge, passion, and dedication to education have had a profound impact on my development as a researcher and a scholar.

July 2023

Ahmad Irham JAMBAK
MSc Student

TABLE OF CONTENTS

Page

ABBREVIATIONS

DOF	**:** Degrees of freedom
P	**:** Proportional
PI	**:** Proportional-Integral
PD	**:** Proportional-Derivative
PID	**:** Proportional-Integral-Derivative
GPS	**:** Global Positioning System
MPC	**:** Model Predictive Control
PPM	**:** Planar Motion Mechanism
NED	**:** North-East-Down
DTC	**:** Duisburg Test Case
CFD	**:** Computational Fluid Dynamics
PSO	**:** Particle Swarm Optimization
GA	**:** Genetic Algorithm
IAE	**:** Integral Absolute Error
ISE	**:** Integral Squared Error
ITAE	**:** Integral Time Absolute Error
ITSE	**:** Integral Time Squared Error

SYMBOLS

X, Y, Z	: Forces with respect to xyz-axes
K, M, N	: Moments with respect to xyz-axes
X′, Y′, Z′	: Nondimensionalized forces with respect to from xyz-axes
m	: Ship's mass
I	: Ship's moment of inertia
$\mathbf{m_x}$, $\mathbf{m_y}$	: Ship added mass
$\mathbf{x_G}$, $\mathbf{y_G}$, $\mathbf{z_G}$	: Ship's center of gravity
u, v, w	: Surge, sway, and heave velocity
U	: Resultant of velocities
p, q, r	: Roll, pitch, and yaw angular velocity
$\boldsymbol{\delta}$	: Rudder angle
$\boldsymbol{\rho}$	: Water density
$\mathbf{t_P}$	: Thrust deduction factor
$\mathbf{n_P}$	: Propeller revolution speed
$\mathbf{D_P}$	: Propeller diameter
$\mathbf{J_P}$	: Propeller advance ratio
$\mathbf{x_P}$	: Propeller position with respect to x-axis
$\mathbf{u_P}$	: Propeller inflow velocity
$\mathbf{w_P}$	: Propeller wake coefficient
$\mathbf{w_{P0}}$	: Propeller wake coefficient in straight motion
$\boldsymbol{\beta_P}$	: Geometrical inflow angle
$\boldsymbol{\beta}$	: Hull drift angle
$\mathbf{K_T}$	: Propeller open water characteristic
$\mathbf{k_0}$, $\mathbf{k_1}$, $\mathbf{k_2}$	: Constants of K_T
$\mathbf{a_H}$	: Rudder force increase factor
$\mathbf{x_H}$	: Longitudinal position of rudder
$\mathbf{t_R}$	: Steering deduction factor
$\mathbf{A_R}$	: Rudder profile area
$\mathbf{U_R}$	: Rudder inflow velocity resultant
$\mathbf{u_R}$, $\mathbf{v_R}$	: Longitudinal and Lateral inflow velocity
$\boldsymbol{\alpha_R}$	: Rudder effective inflow angle
$\boldsymbol{\gamma_R}$	: Flow straightening coefficient
$\boldsymbol{\beta_R}$	: Effective inflow angle to rudder in maneuvering motions
$\mathbf{w_R}$	: Wake coefficient at rudder position
$\mathbf{l_R}$	: Effective longitudinal coordinate
$\mathbf{F_N}$	: Rudder normal force
d	: Longitudinal component of F_N
$\mathbf{L_{PP}}$	: Length of ship
$\boldsymbol{f_\alpha}$	: Rudder lift gradient coefficients
$\boldsymbol{\varepsilon}$	: Ratio of propeller wake fraction and rudder position
$\boldsymbol{\eta}$	: Ratio of propeller diameter to rudder span
$\boldsymbol{\kappa}$	: An experimental constant for expressing u_R

LIST OF TABLES

Page

LIST OF FIGURES

Page

ADDRESSING PARAMETRIC UNCERTAINTIES IN AUTONOMOUS CARGO SHIP HEADING CONTROL

SUMMARY

The progress of computer technology has had a profound influence on the maritime sector, particularly in relation to ship autonomy. The incorporation of computer-assisted systems for guidance, navigation, and control has emerged as a promising approach to minimize the potential risks associated with human errors during ship maneuvering. These errors have the potential to lead to disastrous consequences such as collisions with obstacles, vessel damage, and endangering the safety of passengers and cargo.

Several notable studies have explored ship control systems using different control approaches and conducting simulation-based and real-time implementation tests. These studies include adaptive path following control for accurate target tracking, stabilization of heading angle using cascade control simulations and fuzzy logic-based decision-making mechanisms, integration of sensor information to reduce accidents on common ship routes, collision scenario analysis with fuzzy control-based decision-making aligned with international maritime regulations, design and analysis of planar autonomous position control using two independent propellers, rudder, speed, and position control experiments on a catamaran prototype using a PID approach enhanced by a Kalman Filter, and modeling and real-time control of unmanned surface vehicles with accurate parameter identification. These studies have provided valuable insights and advancements in ship control systems.

Extensive research has also been carried out to address the control of ships with uncertain hydrodynamic coefficients, resulting in the exploration of various approaches. One approach involves using a Multi-level Model Predictive Control (MPC) method to regulate ship speed and calculate propulsion energy while considering uncertainties. Another approach is adaptive control, which continuously adjusts control inputs based on real-time measurements of ship behavior. Fuzzy logic-based control is also utilized, incorporating fuzzy rules that account for uncertainty in hydrodynamic coefficients to adapt the ship's control inputs. Machine learning techniques, like reinforcement learning, are employed to adjust control inputs based on available data. Additionally, robust control techniques are developed to ensure stable and predictable ship behavior even when faced with uncertain hydrodynamic coefficients. These studies make valuable contributions to ship motion control by addressing the challenges associated with uncertain hydrodynamic coefficients and proposing effective control strategies.

This thesis aims to address two significant aspects in the field of ship control. First, the development of a comprehensive ship motion model for the ship's heading angle.

Second, the effective handling of parametric uncertainty in ship hydrodynamics. The research focuses on enhancing the understanding of ship behavior and designing control strategies that can robustly handle uncertainties, ultimately improving the performance, safety, and efficiency of ship operations.

The first objective of this thesis is to construct a control-oriented ship motion model that accurately represents the ship's heading angle dynamics. The model incorporates both linear and nonlinear dynamics to account for the complexities of ship motion under various operating conditions. To derive the linear model, certain assumptions are made to simplify the typical six degrees of freedom (6DOF) equation of motion into a three degrees of freedom (3DOF) equation. From a motion perspective, slow-speed displacement vessels exhibit minimal heave, roll, and pitch motions. Therefore, the variables Z, K, M, and their derivatives, along with the angular velocities w, p, q, can be neglected. From a geometric perspective, conventional ships are symmetrical on the xz-plane. As a result, it is assumed that the y-coordinate of the ship's center of gravity is zero $y_G = 0$.

For the nonlinear model, a well-established 3DOF ship model provided by the Manevering Modelling Group (MMG) is utilized. This model extends the previously derived control-oriented ship equation of motion by incorporating the dynamics of the ship's propeller. By integrating the propeller dynamics into the model, a more comprehensive understanding of the ship's behavior and the interaction between its motion and the propeller can be achieved. The derivations and explanations in this subsection aim to provide valuable insights into the nonlinear ship equation of motion with propeller dynamics, serving as a useful tool for ship motion control design and optimization.

By establishing a reliable ship motion model, it becomes possible to design effective control strategies for heading angle control. This aspect of the research involves reviewing and analyzing existing studies on ship autopilot design, including control methods such as adaptive path following controllers and cascade control simulations. In order to validate the model's accuracy, a turning circle test was conducted. This validation process done by comparing the model's predictions with experimental data from previous studies. To ensure a reliable validation process, a 1/80 scale model of the DTC Container ship was chosen for physical validation. The study's results convincingly demonstrate the model's ability to accurately approximate the trajectory with a fixed rudder angle of $\delta = 35$ degrees. Both the linear and nonlinear models developed in this study exhibit a high level of agreement with the actual system, comparable to the results obtained from other studies utilizing CFD and system-based approaches.

The second objective of this thesis is to address the challenge of parametric uncertainty in ship hydrodynamics, particularly focusing on the uncertainty associated with hydrodynamic coefficients. Hydrodynamic coefficients play a crucial role in understanding the interactions between the ship and the surrounding water. However, these coefficients often exhibit variations due to various factors, such as environmental conditions, vessel modifications, or manufacturing tolerances. The presence of such uncertainty can significantly impact the performance and reliability of ship control systems.

To address this issue, optimization techniques such as Particle Swarm Optimization (PSO) and Genetic Algorithms (GA) have been used to determine the optimal coefficients that best match the ship's motion. However, these methods can be slow, particularly if a large number of samples are needed to represent the uncertainties in the hydrodynamic coefficients. To answer this challenge, this thesis designed a fast optimization algorithm to find a robust optimal controller for ship heading angle control with a certain level of error in hydrodynamic coefficients that is difficult to solve deterministically. The proposed optimization algorithm is referred to as "Bisection Optimization via Blind Search". This methodology involves simulating the model for a total of n samples, utilizing m randomly sampled controller parameters K. The resulting cost value ω is recorded for each simulation. Subsequently, the controller parameter K that produces the lowest ω value is selected. In the second stage, a bisection-based optimization technique is employed to further refine the chosen controller parameter K.

In this thesis, the uncertainty levels considered in this study are set at $\pm 20\%$, representing the permissible deviations of parameters from their nominal values. To mitigate the adverse effects of uncertainty, a simulation scenario is created where the controller is tasked with adjusting the yaw angle ψ from 0 degrees to 40 degrees. To evaluate the optimization performance, four different cost functions are employed: Integral Absolute Error (IAE), Integral Squared Error (ISE), Integral Time Absolute Error (ITAE), and Integral Time Squared Error (ITSE). However, the results indicate that the optimal controller parameters obtained using these different cost functions do not exhibit significant differences. Two types of controllers, namely proportional (P) and proportional-derivative (PD) controllers, are investigated in this study. The inclusion of the derivative term in the PD controller aims to mitigate oscillations and overshoot in the system's response, thereby improving stability and settling time. However, the integral term is excluded from consideration due to the inherent stability of the system and its expected slow response. The results demonstrate that the proposed algorithm outperforms existing methods such as Particle Swarm Optimization (PSO) in terms of both execution speed and task performance.

By achieving these 2 objectives, this thesis contributes to the field of ship control by providing a comprehensive understanding of ship motion dynamics and offering effective solutions for addressing parametric uncertainty in ship hydrodynamics. The outcomes of this research can significantly impact various maritime applications, including autonomous navigation, collision avoidance, and energy-efficient ship operations. The developed ship motion model and the proposed optimization approaches can be implemented in real-world scenarios, enabling improved control strategies for ship heading angle control and enhancing the overall performance and safety of ship operations.

In conclusion, this thesis combines the development of a control-oriented ship motion model with the effective handling of parametric uncertainty in ship hydrodynamics. The research contributes to the advancement of ship control by providing valuable insights, methodologies, and tools that can be utilized in designing robust control strategies for ship heading angle control under uncertain operating conditions. The findings of this thesis have the potential to enhance the efficiency, safety, and sustainability of ship operations, ultimately benefiting the maritime industry as a whole.

OTONOM KARGO GEMİSİ YÖN KONTROLÜNDEKİ PARAMETRİK BELİRSİZLİKLERİN ELE ALINMASI

ÖZET

Bilgisayar teknolojisindeki ilerlemenin, özellikle gemi özerkliği ile ilgili olarak, denizcilik sektörü üzerinde derin bir etkisi olmuştur. Kılavuzluk, navigasyon ve kontrol için bilgisayar destekli sistemlerin dahil edilmesi, gemi manevrası sırasında insan hatalarıyla ilişkili potansiyel riskleri en aza indirmek için umut verici bir yaklaşım olarak ortaya çıkmıştır. Bu hatalar, engellerle çarpışma, gemi hasarı, yolcu ve yük güvenliğini tehlikeye atma gibi feci sonuçlara yol açma potansiyeline sahiptir.

Birkaç önemli çalışma, farklı kontrol yaklaşımları kullanan ve simülasyona dayalı ve gerçek zamanlı uygulama testleri yürüten gemi kontrol sistemlerini araştırmıştır. Bu çalışmalar, doğru hedef takibi için uyarlanabilir yol takip kontrolü, kademeli kontrol simülasyonları ve bulanık mantık tabanlı karar verme mekanizmaları kullanılarak rota açısının stabilizasyonu, ortak gemi rotalarında kazaları azaltmak için sensör bilgilerinin entegrasyonu, bulanık kontrol tabanlı çarpışma senaryosu analizi içerir. uluslararası denizcilik yönetmeliklerine uygun karar verme, iki bağımsız pervane kullanılarak düzlemsel otonom konum kontrolünün tasarımı ve analizi, bir Kalman Filtresi ile geliştirilmiş bir PID yaklaşımı kullanan bir katamaran prototipi üzerinde dümen, hız ve konum kontrolü deneyleri ve modelleme ve gerçek zamanlı doğru parametre tanımlaması ile insansız yüzey araçlarının kontrolü. Bu çalışmalar, gemi kontrol sistemlerinde değerli bilgiler ve ilerlemeler sağlamıştır.

Belirsiz hidrodinamik katsayılara sahip gemilerin kontrolünü ele almak için kapsamlı araştırmalar da yapılmış ve bu da çeşitli yaklaşımların araştırılmasına yol açmıştır. Bir yaklaşım, belirsizlikleri göz önünde bulundurarak gemi hızını düzenlemek ve sevk enerjisini hesaplamak için Çok Seviyeli Model Predictive Control (MPC) yöntemini kullanmayı içerir. Diğer bir yaklaşım ise, gemi davranışının gerçek zamanlı ölçümlerine dayalı olarak kontrol girdilerini sürekli olarak ayarlayan uyarlamalı kontroldür. Geminin kontrol girdilerini uyarlamak için hidrodinamik katsayılardaki belirsizliği açıklayan bulanık kuralları içeren bulanık mantık tabanlı kontrol de kullanılır. Takviyeli öğrenme gibi makine öğrenimi teknikleri, mevcut verilere dayalı olarak kontrol girdilerini ayarlamak için kullanılır. Ek olarak, belirsiz hidrodinamik katsayılarla karşı karşıya kalındığında bile kararlı ve öngörülebilir gemi davranışı sağlamak için sağlam kontrol teknikleri geliştirilmiştir. Bu çalışmalar, belirsiz hidrodinamik katsayılarla ilgili zorlukları ele alarak ve etkili kontrol stratejileri önererek gemi hareket kontrolüne değerli katkılar sağlar.

Bu tez, gemi kontrolü alanındaki iki önemli yönü ele almayı amaçlamaktadır. İlk olarak, geminin pruva açısı için kapsamlı bir gemi hareket modelinin geliştirilmesi.

İkincisi, gemi hidrodinamiğindeki parametrik belirsizliğin etkili bir şekilde ele alınması. Araştırma, gemi davranışının anlaşılmasını geliştirmeye ve belirsizlikleri sağlam bir şekilde ele alabilecek kontrol stratejileri tasarlamaya, sonuçta gemi operasyonlarının performansını, güvenliğini ve verimliliğini geliştirmeye odaklanıyor.

Bu tezin ilk amacı, geminin yön açısı dinamiklerini doğru bir şekilde temsil eden, kontrol yönelimli bir gemi hareket modeli oluşturmaktır. Model, çeşitli çalışma koşulları altında gemi hareketinin karmaşıklığını hesaba katmak için hem doğrusal hem de doğrusal olmayan dinamikleri birleştirir. Doğrusal modeli türetmek için, tipik 6 Degrees of Freedom (6DOF) hareket denklemini 3 Degrees of Freedom (3DOF) denklemine basitleştirmek için belirli varsayımlar yapılır. Hareket perspektifinden bakıldığında, yavaş hızlı yer değiştiren gemiler minimum kaldırma, yalpalama ve yunuslama hareketleri sergiler. Bu nedenle Z, K, M değişkenleri ve bunların türevleri, açısal hızlar w, p, q ile birlikte ihmal edilebilir. Geometrik bir perspektiften bakıldığında, geleneksel gemiler xz düzleminde simetriktir. Sonuç olarak, geminin ağırlık merkezinin y-koordinatının sıfır $y_G = 0$ olduğu varsayılır.

Doğrusal olmayan model için, Manevering Modeling Group (MMG) tarafından sağlanan köklü bir 3DOF gemi modeli kullanılmıştır. Bu model, geminin pervanesinin dinamiklerini dahil ederek önceden türetilen kontrol yönelimli gemi hareket denklemini genişletir. Pervane dinamiklerini modele entegre ederek, geminin davranışı ve hareketi ile pervane arasındaki etkileşim hakkında daha kapsamlı bir anlayış elde edilebilir. Bu alt bölümdeki türetmeler ve açıklamalar, gemi hareket kontrol tasarımı ve optimizasyonu için yararlı bir araç olarak hizmet ederek pervane dinamiği ile doğrusal olmayan gemi hareket denklemi hakkında değerli bilgiler sağlamayı amaçlamaktadır.

Güvenilir bir gemi hareket modeli oluşturarak, rota açısı kontrolü için etkili kontrol stratejileri tasarlamak mümkün hale gelir. Araştırmanın bu yönü, uyarlanabilir yol takip kontrolörleri ve kademeli kontrol simülasyonları gibi kontrol yöntemleri dahil olmak üzere, gemi otopilot tasarımına ilişkin mevcut çalışmaların gözden geçirilmesini ve analiz edilmesini içerir. Modelin doğruluğunu doğrulamak için bir dönüş çemberi testi yapılmıştır. Bu doğrulama işlemi, modelin tahminlerini önceki çalışmalardan elde edilen deneysel verilerle karşılaştırarak yapılır. Güvenilir bir doğrulama süreci sağlamak için, fiziksel doğrulama için DTC Konteyner gemisinin 1/80 ölçekli bir modeli seçildi. Çalışmanın sonuçları, modelin $\delta = 35$ derecelik sabit bir dümen açısı ile yörüngeye doğru bir şekilde yaklaşma yeteneğini ikna edici bir şekilde göstermektedir. Bu çalışmada geliştirilen hem doğrusal hem de doğrusal olmayan modeller, CFD ve sistem tabanlı yaklaşımları kullanan diğer çalışmalardan elde edilen sonuçlarla karşılaştırılabilir şekilde, gerçek sistemle yüksek düzeyde bir uyum sergiler.

Bu tezin ikinci amacı, özellikle hidrodinamik katsayılarla ilişkili belirsizliğe odaklanarak, gemi hidrodinamiğindeki parametrik belirsizliğin zorluğunu ele almaktır. Hidrodinamik katsayılar, gemi ve çevredeki su arasındaki etkileşimlerin anlaşılmasında çok önemli bir rol oynar. Bununla birlikte, bu katsayılar genellikle çevresel koşullar, kap modifikasyonları veya üretim toleransları gibi çeşitli faktörlere bağlı olarak farklılıklar gösterir. Bu tür bir belirsizliğin varlığı, gemi kontrol sistemlerinin performansını ve güvenilirliğini önemli ölçüde etkileyebilir.

Bu sorunu ele almak için, geminin hareketine en iyi uyan optimum katsayıları belirlemek için Particle Swarm Optimization (PSO) ve Genetic Algorithm (GA)

gibi optimizasyon teknikleri kullanılmıştır. Bununla birlikte, özellikle hidrodinamik katsayılardaki belirsizlikleri temsil etmek için çok sayıda numuneye ihtiyaç duyuluyorsa, bu yöntemler yavaş olabilir. Bu zorluğa cevap vermek için bu tez, hidrodinamik katsayılarda deterministik olarak çözülmesi zor olan belirli bir hata düzeyine sahip gemi rota açısı kontrolü için sağlam bir optimal kontrolör bulmak üzere hızlı bir optimizasyon algoritması tasarladı. Önerilen optimizasyon algoritmasına "Bisection Optimization via Blind Search " adı verilir. Bu metodoloji, rastgele örneklenen m denetleyici parametreleri K kullanılarak toplam n örnek için modelin simüle edilmesini içerir. Ortaya çıkan maliyet değeri ω, her simülasyon için kaydedilir. Ardından, en düşük ω değerini üreten denetleyici parametresi K seçilir. İkinci aşamada, seçilen denetleyici parametresi K'yi daha da hassaslaştırmak için ikiye bölmeye dayalı bir optimizasyon tekniği kullanılır.

Bu tezde, bu çalışmada ele alınan belirsizlik seviyeleri, parametrelerin nominal değerlerinden izin verilen sapmalarını temsil eden $\pm 20\%$ olarak belirlenmiştir. Belirsizliğin olumsuz etkilerini azaltmak için, kontrolörün sapma açısını ψ 0 dereceden 40 dereceye ayarlamakla görevlendirildiği bir simülasyon senaryosu oluşturulur. Optimizasyon performansını değerlendirmek için dört farklı maliyet fonksiyonu kullanılır: Integral Absolute Error (IAE), Integral Squared Error (ISE), Integral Time Absolute Error (ITAE), ve Integral Time Squared Error (ITSE). Ancak sonuçlar, bu farklı maliyet fonksiyonları kullanılarak elde edilen optimal denetleyici parametrelerinin önemli farklılıklar göstermediğini göstermektedir. Bu çalışmada Proportional (P) ve Proportional-Derivative (PD) olmak üzere iki tip kontrolör incelenmiştir. Türev teriminin PD kontrolörüne dahil edilmesi, sistemin tepkisindeki salınımları ve aşmaları azaltmayı ve böylece kararlılığı ve oturma süresini iyileştirmeyi amaçlar. Bununla birlikte, sistemin doğal kararlılığı ve beklenen yavaş tepkisi nedeniyle integral terimi dikkate alınmaz. Sonuçlar, önerilen algoritmanın hem yürütme hızı hem de görev performansı açısından PSO gibi mevcut yöntemlerden daha iyi performans gösterdiğini göstermektedir.

Bu 2 hedefe ulaşarak, bu tez, gemi hareket dinamikleri hakkında kapsamlı bir anlayış sağlayarak ve gemi hidrodinamiğindeki parametrik belirsizliği ele almak için etkili çözümler sunarak gemi kontrolü alanına katkıda bulunur. Bu araştırmanın sonuçları, otonom navigasyon, çarpışmadan kaçınma ve enerji tasarruflu gemi operasyonları dahil olmak üzere çeşitli denizcilik uygulamalarını önemli ölçüde etkileyebilir. Geliştirilen gemi hareket modeli ve önerilen optimizasyon yaklaşımları, gerçek dünya senaryolarında uygulanarak gemi rota açısı kontrolü için geliştirilmiş kontrol stratejileri sağlar ve gemi operasyonlarının genel performansını ve güvenliğini artırır.

Sonuç olarak, bu tez, gemi hidrodinamiğindeki parametrik belirsizliğin etkili bir şekilde ele alınması ile kontrol odaklı bir gemi hareket modelinin geliştirilmesini birleştirir. Araştırma, belirsiz çalışma koşulları altında gemi yön açısı kontrolü için sağlam kontrol stratejileri tasarlamada kullanılabilecek değerli içgörüler, metodolojiler ve araçlar sağlayarak gemi kontrolünün ilerlemesine katkıda bulunur. Bu tezin bulguları, gemi operasyonlarının verimliliğini, güvenliğini ve sürdürülebilirliğini artırma potansiyeline sahiptir ve sonuçta bir bütün olarak denizcilik endüstrisine fayda sağlar.

1. INTRODUCTION

The advancements in computer technology have significantly impacted the maritime industry, particularly in the area of ship autonomy. The integration of computer-assisted guidance, navigation, and control systems come out to be an effective approach in order to mitigate the risk of human errors during ship maneuvering [1]. Potential disaster from human error during maneuver are collisions with obstacles, damage to the ship, and pose risks to the safety of passengers and cargo [2].

Several notable studies, specifically to ship control systems, are done by utilizing various control approaches and conducting both simulation-based and real-time implementation tests. Zhang et al. [3] proposed an adaptive path following controller that enables a ship model to accurately track specified target points. Ahmed and Hasegawa [4] investigated the stabilization of the heading angle in a ship model with three degrees-of-freedom (DOF) using a cascade control simulation approach. The study incorporates fuzzy logic-based decision-making mechanisms to update controller coefficients, ensuring stability during maneuvering between waypoints. Sandler et al. [5] have focused on reducing accidents on frequently used ship routes by integrating information from various sensors on different ship types. Moreover, Perera [6] has explored ship collision scenarios under different external factors, employing a decision-making method based on fuzzy control principles aligned with international maritime regulations. Reyhanoglu [7] has conducted in-depth research on the design and mathematical analysis of planar autonomous position control using two independent propellers. Additionally, Caccia et al. [8] have carried out rudder, speed, and position control experiments on a catamaran prototype using compass and GPS information, with control based on a proportional-integral-derivative (PID) approach enhanced by the implementation of a Kalman Filter. Sonnenburg and Woolsey [9] have focused on modeling an unmanned surface vehicle, accurately identifying real system parameters and controlling it in real time.

The control of ships with uncertain hydrodynamic coefficients has also been a subject of significant researches. Several approaches have been explored to address this challenge. Haseltalab et al. [10] proposed a Multi-level Model Predictive Control (MPC) method to control ship speed and calculate propulsion energy in the presence of uncertainties. Lu et al. [11] pursued an adaptive control approach, continuously adjusting control inputs based on real-time measurements of ship behavior. Chen and Tan [12] utilized fuzzy logic-based control, incorporating fuzzy rules that consider uncertainty in hydrodynamic coefficients to adjust the ship's control inputs. Machine learning-based techniques have also been employed, such as the reinforcement learning method proposed by Zhang et al. [13], which adjusts control inputs based on available data. Furthermore, robust control techniques have been developed to ensure stable and predictable ship behavior despite uncertain hydrodynamic coefficients, as demonstrated by Ye et al. [14]. These studies collectively contribute to the body of knowledge in ship motion control by addressing the challenges posed by uncertain hydrodynamic coefficients and proposing effective control strategies.

1.1 Aim and Purpose of Thesis

The purpose of this thesis is two-fold. Firstly, it aims to develop a comprehensive and control-oriented ship motion model for the ship's heading angle. This involves the modeling of both linear and nonlinear dynamics to accurately represent the behavior of the ship's heading angle under various operating conditions. By constructing a reliable ship motion model, this research intends to facilitate the design and implementation of effective control strategies for ship heading angle control.

Secondly, this thesis seeks to address the challenge of parametric uncertainty, particularly focusing on the uncertainties associated with hydrodynamic coefficients. Accuracy of hydrodynamic coefficients play a crucial role in characterizing the complex interactions between the ship and the surrounding water. However, these coefficients often exhibit variations due to factors such as environmental conditions, vessel modifications, or manufacturing tolerances. The presence of such uncertainty can significantly affect the performance and reliability of ship control systems. Hence, this research aims design a controller through optimization approaches that effectively

account for parametric uncertainty in ship hydrodynamics. This enable the design of control strategies that are robust against these uncertainties.

By achieving these objectives, this thesis aims to contribute to the field of ship control by providing valuable insights into the modeling and control of ship motion and also offering effective solutions to mitigate the impact of parametric uncertainty in ship hydrodynamics. Ultimately, the outcomes of this research endeavor aim to enhance the performance, safety, and efficiency of ship operations in various maritime applications.

1.2 Outline of Thesis

The thesis is structured into several chapters to ensure a systematic and comprehensive study of ship motion control. Chapter 2 serves as an introduction of of autonomous ships, their components, and recent developments in the field. In Chapter 3, the focus shifts to the modeling of ship motion, encompassing both linear and nonlinear approaches. These models are rigorously validated using the Turning Circle test, allowing for a meticulous comparison with existing studies and experimental results from real systems. Building upon this foundation, Chapter 4 delves into the explanation and implementation of a PID-based controller for ship heading tracking. Through a detailed examination of proportional, proportional-derivative, and proportional-integral-derivative (PID) controllers, the suitability of each approach for ship motion control applications is assessed. Moving forward, Chapter 5 confronts the complex challenge of addressing uncertainty in ship hydrodynamics. The problem formulation is presented, accompanied by a proposed method for managing parametric uncertainty. The effectiveness of this method is thoroughly evaluated through a series of meticulously designed test cases, thereby demonstrating its ability to effectively handle uncertainty and enhance ship motion control. Ultimately, Chapter 6 provides a cohesive conclusion, summarizing the key findings and contributions of the thesis. It highlights the main insights gained throughout the study and discusses potential avenues for future research and improvement in the field of ship motion control.

2. OVERVIEW OF SHIP MOTION

2.1 Ship Motions in General

Ship motions are essential aspects of understanding its behavior at sea. These motions can be categorized into rotational and translational motions, each associated with specific axes and effects. This subchapter provides an overview motions experienced by ships.

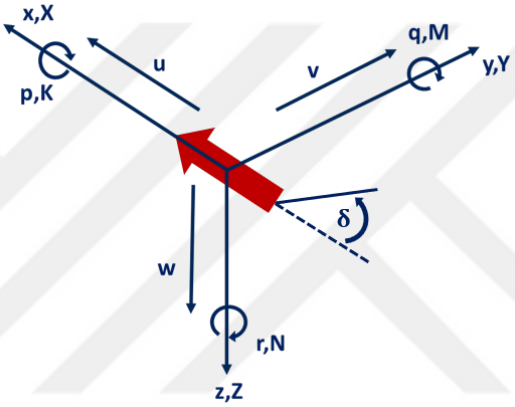

Figure 2.1 : Ship motion: axes, rotational, and translational.

The rotational motions of a ship occur around the longitudinal, transverse, and vertical axes. The longitudinal axis, also known as the X axis, runs from bow to stern and is associated with the roll motion [15]. Roll refers to the tilting rotation of the vessel around its longitudinal axis [16]. Roll can be intentional or unintentional, caused by factors such as wind pressure, turning, or shifting cargo. The transverse axis, denoted as the Y axis, extends from side to side and corresponds to the pitch motion. Pitch involves the up-and-down rotation of the vessel around its transverse axis [17]. Trim or out of trim describes any deviation from the normal pitch position. The vertical axis, known as the Z axis, represents the yaw motion. Yaw refers to the turning rotation of the vessel around its vertical axis. Deviations from the normal yaw position affect the heading of the boat [18].

In addition to rotational motions, ships also experience translational movements. Surge, which occurs along the longitudinal axis X, is a linear front-to-back or

bow-to-stern motion [19]. It is influenced by the sea conditions as well as propulsion system accelerations. Sway, on the other hand, is a linear side-to-side or port-to-starboard motion associated with the transverse axis Y. It can be generated by water and wind forces acting on the hull, lateral wave motion, or the ship's own propulsion [20]. Sway can also be induced indirectly by the ship's inertia during turning maneuvers, resulting in a lateral drift from the vessel's intended course. Heave represents the linear vertical motion of the ship, involving upward and downward displacements [21].

2.2 Evaluation of Ship Motion

In the field of marine engineering, ship motion evaluation is a hydrodynamic test conducted to evaluate ship new design or refine existing ship designs for improved performance at sea. These tests take place in a dedicated facility known as a ship model basin or towing tank. Various types of tests are carried out, including straight line tests, rotating-arm technique tests, and planar motion mechanism tests, which provide valuable insights into a ship's behavior.

2.2.1 Straight line test

Figure 2.2 shows a straight line test [22]. During the test, ship model is towed along a straight path in the towing tank at a constant velocity, corresponding to a specific Froude number for the ship [23]. The model is subjected to different angles of attack, and a dynamometer measures the forces Y and moments N experienced by the model at each angle. By analyzing these measurements, the velocity-dependent derivatives (Y_v and N_v) of the ship can be determined [24]. These dimensional ship values are obtained by multiplying the non-dimensional derivatives by appropriate combinations of ship length, speed, and water density.

Figure 2.2 : Straight line test conducted by Davidson Laboratory.

2.2.2 Rotating-arm technique

The rotating-arm technique, as shown in Figure 2.3, involves a specialized towing tank apparatus called a rotating-arm facility [25]. In this setup, the ship model is fixed to the end of a radial arm and rotated about a vertical axis within the tank [26]. As the model revolves, it experiences an imposed angular velocity (yaw rate). By measuring the forces Y and moments N acting on the model, the rotary derivatives (Y_r and N_r) can be determined. Additionally, cross-plotting the values of Y_v and N_v obtained at different radii enables the calculation of Y_v and N_v at the center $r = 0$ of rotation [27].

Figure 2.3 : Rotating-Arm test conducted at Krylov State Research Centre.

2.2.3 Planar motion mechanism (PMM)

Figure 2.4 illustrates the Planar motion mechanism (PMM) test [28]. This test is an alternative to the rotating arm test, particularly useful in longer and narrower towing tanks. It measures velocity-dependent derivatives (Y_v and N_v), rotary derivatives (Y_r and N_r), as well as acceleration derivatives (Y'_v and N'_v) [28]. The PMM consists of

two oscillators—one producing transverse oscillations at the bow and the other at the stern [29]. As the model moves down the towing tank at a constant velocity along the centerline, these oscillations provide valuable data on the ship's characteristics.

Figure 2.4 : Planar Motion Mechanism test.

2.3 Seakeeping Factors

Seakeeping performance, which refers to how a ship responds to the surrounding waves, is influenced by several factors that play a crucial role in determining its behavior at sea. These factors need to be carefully considered and understood to assess and optimize a ship's seakeeping capabilities. One significant factor is the size of the ship. Generally, larger vessels tend to experience lower motions compared to smaller ones due to the relatively smaller size of the waves they encounter [30]. The displacement, or weight, of a ship also plays a role [31]. Heavier ships typically have lower motions than lighter ones since greater mass results in lower accelerations when subjected to the same wave energy.

Stability is another critical factor affecting seakeeping [32]. A ship's stability determines how closely it follows the wave profile. More stable ships tend to track the waves more accurately, resulting in higher accelerations but lower amplitudes of motion. Additionally, the freeboard of a vessel, which is the vertical distance between the waterline and the main deck, influences its seakeeping performance [33]. Ships with greater freeboard are less likely to immerse their decks in waves, which is an important criterion for various types of vessels. Human factors also play a significant role in seakeeping, especially in smaller vessels [34].

3. CONTROL-ORIENTED CARGO SHIP MOTION MODEL

The development of effective control strategies is crucial for ensuring safe and efficient ship operations. In order to obtain such effective controller, a reliable so called "control-oriented" ship motion model that captures the dynamic behavior of cargo ships is essential. This chapter presents a comprehensive discussion on the designing a control-oriented cargo ship motion model. The model aims to provide a mathematical representation of the ship's motion that enables accurate analysis and implementation of control strategies which can led to a better performance.

The cargo ship motion model discussed in this chapter focuses on capturing the key dynamics in 3DOF (degrees of freedom) that are relevant for control purposes. The motion model allows for the analysis of the ship's behavior in terms of surge, sway, and yaw of the ship. These motions, as mentioned in the previous chapter, can provide valuable insights into the ship's response to control inputs and external disturbances. Within this chapter, an overview of cargo ship hydrodynamics and the principles governing ship motion will also be provided. The subsequent discussion will delve into the details of the control-oriented modifications made to the ship equation of motion to tailor it specifically for control strategies and optimization approaches.

The control-oriented cargo ship motion model is essential to facilitate the development and evaluation of various control strategies and optimization approaches, as further discussed in subsequent chapters. By understanding and utilizing this motion model, researchers and engineers can explore advanced control techniques and optimize the ship's performance. Through this chapter, a solid foundation will be established for the subsequent discussions on control strategies and optimization approaches in cargo ship motion control.

3.1 Linear Motion Model

Linear ship equation of motion is a fundamental in ship hydrodynamics and motion control model. It provides a simplified representation of a ship's motion by considering its surge, sway, and yaw degrees of freedom. This subchapter aims to provide a comprehensive understanding of the 3 Degree-of-Freedom (DOF) linear ship equation of motion and its significance in ship motion control.

The linearized ship motion kinematics and dynamics model is derived the following 6-DOF Equations. The equations of motion [35]:

$$m[\dot{u} - rv + wq - x_G\left(q^2 + r^2\right) + y_G\left(pq - \dot{r}\right) + z_G\left(pr + \dot{q}\right)] = X \tag{3.1a}$$

$$m[\dot{v} - wp + ur - y_G\left(r^2 + p^2\right) + z_G\left(qr - \dot{p}\right) + x_G\left(qp + \dot{r}\right)] = Y \tag{3.1b}$$

$$m[\dot{w} - uq + vp - z_G\left(p^2 + q^2\right) + x_G\left(rp - \dot{q}\right) + y_G\left(rq + \dot{p}\right)] = Z \tag{3.1c}$$

as force equations, and

$$I_x\dot{p} + \left(I_z - I_y\right)qr + m\left[y_G\left(\dot{w} - uq + vp\right) - z_G\left(\dot{v} - wp + ur\right)\right] = K \tag{3.2a}$$

$$I_y\dot{q} + \left(I_x - I_z\right)rp + m\left[z_G\left(\dot{u} - vr + wq\right) - x_G\left(\dot{w} - uq + vp\right)\right] = M \tag{3.2b}$$

$$I_z\dot{r} + \left(I_y - I_x\right)pq + m\left[x_G\left(\dot{v} - wp + ur\right) - y_G\left(\dot{u} - vr + wq\right)\right] = N \tag{3.2c}$$

as moment equations, where u, v, w are surge, sway and heave velocities; p, q, r are roll, pitch, and yaw rates; x_G, y_G, z_G are x, y, z coordinates of the center of gravity; m and I are mass and moment of inertia; X, Y, Z are forces to generate surge, sway and heave motions; and K, M, N are moments to generate roll, pitch and yaw motions. Equations (3.1) represents the translational motions of the ship while (3.2) are for rotational motions. Notably, the variables u, v, w, p, q, r are in the body-fixed frame, while x, y, z are in the global North-East-Down (NED) frame, necessitating frame transformation.

From the motion perspective, slow-speed displacement vessels do not have significant heave, roll and pitch motions. Thus, Z, K, M and w, p, q along with their derivatives can be neglected [36]. From the geometric perspective, conventional ships are symmetrical on the xz plane. Therefore, it can be assumed that the y-coordinate of the center of gravity is equal to zero, $y_G = 0$. Using these assumptions, (3.1a) - (3.2c) simplified to 3 DOF as follows:

$$m(\dot{u} - rv - x_G r^2) = X \tag{3.3a}$$

$$m(\dot{v} + r + x_G \dot{r}) = Y \tag{3.3b}$$

$$I_z \dot{r} + m x_G (\dot{v} + r) = N \tag{3.3c}$$

Now that the assumptions of the model are defined, the nonlinearities in (3.3) need to be addressed. There are two nonlinear terms rv and r^2. These two terms can be neglected because both r and v are small numbers so the multiplication of both of them can be approximated to 0. The resulting equations are as follows:

$$m\dot{u} = X \tag{3.4a}$$

$$m[\dot{v} + r + x_G \dot{r}] = Y \tag{3.4b}$$

$$I_z \dot{r} + m x_G (\dot{v} + r) = N \tag{3.4c}$$

Notice that all of the terms on the left-hand side are defined but the ones on the right-hand side are not. In order to have (3.4) written purely in terms of the state variables $u, v, r, \dot{u}, \dot{v}, \dot{r}$ and input variable δ, where δ denotes the rudder angle, the terms X, Y, N are expressed in terms of these state and input variables using Taylor's Series Expansion. The number of hydrodynamic coefficients in a generic Taylor's Series Expansion depends on the order of nonlinearity to be considered [3, 5]. We use a linearized model in this study; therefore, we only consider the first-order terms. Hence we have:

$$X \approx X_{\dot{u}}\dot{u} + X_u u + X_{\dot{v}}\dot{v} + X_v v + X_{\dot{r}}\dot{r} + X_r r + X_\delta \delta \tag{3.5a}$$

$$Y \approx Y_{\dot{u}}\dot{u} + Y_u u + Y_{\dot{v}}\dot{v} + Y_v v + Y_{\dot{r}}\dot{r} + Y_r r + Y_\delta \delta \tag{3.5b}$$

$$N \approx N_{\dot{u}}\dot{u} + N_u u + N_{\dot{v}}\dot{v} + N_v v + N_{\dot{r}}\dot{r} + N_r r + N_\delta \delta \tag{3.5c}$$

Some of the coefficients stated in (3.5) are not significantly affecting the ship during maneuver. Therefore, they can be neglected reducing the force and moment equations as follows:

$$X \approx X_{\dot{u}}\dot{u} + X_u u + + X_\delta \delta \tag{3.6a}$$

$$Y \approx Y_{\dot{v}}\dot{v} + Y_v v + Y_{\dot{r}}\dot{r} + Y_r r + Y_\delta \delta \tag{3.6b}$$

$$N \approx N_{\dot{v}}\dot{v} + N_v v + N_{\dot{r}}\dot{r} + N_r r + N_\delta \delta \tag{3.6c}$$

When we substitute (3.6) into (3.4) respectively, and then move all the added mass relates terms to the left-hand side, the equations of motion for the ship are obtained as follows:

$$(m - X_{\dot{u}})\,\dot{u} = X_u u + X_\delta \delta \tag{3.7a}$$

$$(m - Y_{\dot{v}})\,\dot{v} + (mx_G - Y_{\dot{r}})\,\dot{r} = (Y_v - m)v + (Y_r - mU)\,r + Y_\delta \delta \tag{3.7b}$$

$$(mx_G - N_{\dot{v}})\,\dot{v} + (I_z - N_{\dot{r}})\,\dot{r} = N_v v + (N_r - mx_G U)\,r + N_\delta \delta \tag{3.7c}$$

The thrust generated by a propeller considered to be equal to K_T/J^2, where K_T denotes propeller thrust open water characteristic and J is propeller advanced ratio, as explained in [37, 38]. The propeller model considers only the thrust force generated by the propeller. Side forces and moments are completely ignored [39]. The propeller thrust force X_P is added to the the right-hand side of surge equation (3.7a). The new ship surge motion equation becomes:

$$(m - X_{\dot{u}})\,\dot{u} = X_u u + X_\delta \delta + X_P \tag{3.8}$$

The surge force due to the thrust generated by the propeller is given by the equation:

$$X_P = (1 - t_P)\,T_p \tag{3.9}$$

Where t_P is the thrust deduction factor and T_p is the propeller thrust. The details of propeller modeling can be found in [40]; however, the equations used in this propeller model are summarized in Table 1 for the completeness of this study.

Table 3.1 : Equations required to calculate the hydrodynamic force of the propeller.

Definition	Equation
Thrust of propeller	$T_p = \rho n_P^2 D_P^4 K_T$
Thrust coefficient	$K_T = k_0 + k_1 J_P + k_2 J_P^2$
Propeller advance ratio	$J_P = u_P / n_P D_P$
Inflow velocity to propeller	$u_P = u(1 - w_P)$
Wake fraction of propeller	$w_P = w_{P0} \exp(-4\beta_P^2)$
Geometrical inflow angle	$\beta_P = \beta - x'_P r'$

3.2 Nonlinear Motion Model

This subsection focuses on the derivation and analysis of the Maneuver Modeling Group (MMG) model [40], a well-established 3DOF nonlinear ship equation of motion. The MMG model extends the previously derived control-oriented ship equation of motion by incorporating the dynamics of the ship propeller. By integrating the propeller dynamics into the model, a more comprehensive understanding of the ship's behavior and the interaction between its motion and the propeller can be obtained. The derivations and explanations presented in this subsection aim to provide insights into the nonlinear ship equation of motion with propeller dynamics, which serves as a valuable tool for ship motion control design and optimization.

The derivation process for transitioning from a 6-DOF to a 3-DOF nonlinear ship equation is initially similar to that of the linear equation, as discussed in the preceding subsection. A key point of difference occurs from (3.3). At this juncture, each component—namely, the surge force X, sway force Y, and yaw moment N—is formulated as follows:

$$X = X_H + X_R + X_P \tag{3.10a}$$

$$Y = Y_H + Y_R \tag{3.10b}$$

$$N = N_H + N_R \tag{3.10c}$$

The use of subscripts H, R, and P signifies the hydrodynamic forces and moment generated by main parts of the ship, namely the hull, rudder, and propeller.

3.2.1 Forces and moment acting on the hull

The forces and moment exerted on the ship hull, denoted as X_H, Y_H, and N_H, can be represented by the following polynomial expressions:

$$X'_H(v'_m, r\prime) = -R'_0 + X'_{vv}v'^2_m + X'_{vr}v'_m r\prime + X'_{rr}r'^2 + X'_{vvvv}v'^4_m \tag{3.11a}$$

$$Y'_H(v'_m, r\prime) = Y'_v v'_m + Y'_R r\prime + Y'_{vvv}v'^3_m + Y'_{vvr}v'^2_m r' + Y'_{vrr}v'_m r'^2 + Y'_{rrr}r'^3 \tag{3.11b}$$

$$N'_H(v'_m, r\prime) = N'_v v'_m + N'_R r\prime + N'_{vvv}v'^3_m + N'_{vvr}v'^2_m r' + N'_{vrr}v'_m r'^2 + N'_{rrr}r'^3 \tag{3.11c}$$

where all of the subscripted $X\prime$, $Y\prime$, and $N\prime$ variables on the right-hand side are the hydrodynamics derivative on maneuvering. The prime accents denote nondimensionalized unit. Nondimensionalizing the units in ship hydrodynamics is essential to simplify and generalize the analysis of ship behavior across different scales and conditions. By removing the influence of specific units, we can express relationships and parameters in dimensionless form, allowing for more universal comparisons and generalizations [41]. This approach enables researchers and engineers to develop standardized models and design principles that can be applied to various ship sizes, speeds, and environmental conditions. Forces and moment acting on the hull can be nondimensionalized as follows:

$$X_H = \frac{\rho L_{pp} d U^2 X'_H(v'_m, r\prime)}{2} \tag{3.12a}$$

$$Y_H = \frac{\rho L_{pp} d U^2 Y'_H(v'_m, r\prime)}{2} \tag{3.12b}$$

$$N_H = \frac{\rho L_{PP}^2 d U^2 N'_H(v'_m, r\prime)}{2} \tag{3.12c}$$

3.2.2 Force acting on propeller

A cargo ship propeller is a crucial component of marine propulsion systems used in large merchant vessels designed for transporting goods. It is a rotating device that converts the mechanical power generated by the ship's engine into thrust, propelling the vessel through the water. The MMG model considers the propeller's effect only on the surge motion of the ship which outlined in equation (3.10). The generated a surge force X_P influences the forward or backward motion of the vessel. The calculation of X_P is determined according to the following equation:

$$X_P = (1 - t_P)T \tag{3.13}$$

In order to simplify the analysis, the MMG model assumes that the thrust deduction factor t_P to remain constant for a given propeller load. The propeller thrust T can be calculated as follows:

$$T = \rho n_p^2 D_P^2 K_T(J_P) \tag{3.14}$$

Here, T is determined by several factors. These factors include the propeller revolution rate n_P, the propeller diameter D_P, and the propeller thrust open water characteristic

K_T. In MMG model, K_T is approximated in term of Propeller advanced ratio J_P which expressed set of following equations:

$$K_T(J_P) = k_2 J_P^2 + k_1 J_P + k_0 \tag{3.15}$$

The coefficients k_0, k_1, and k_2 represent the parameters associated with K_T. The calculation of J_P model is carried out as follows:

$$J_P = \frac{u_P}{n_P D_P} \tag{3.16}$$

The inflow velocity to the propeller u_P, is determined based on the following calculation equation:

$$u_P = u(1 - w_P) \tag{3.17}$$

where the wake coefficient at the propeller position during maneuvering motions w_P, is determined as follows:

$$w_P = w_{P0} \exp(-4\beta_P^2) \tag{3.18}$$

In (3.18), w_{P0} denotes ship's wake coefficient at propeller position in straight moving while β_P denote geometrical inflow angle to propeller in maneuvering motions which can be expressed as:

$$\beta_P = \beta - x'_P r' \tag{3.19}$$

Here, β_P computed by subtracting the hull drift angle at mid-ship β with multiplication of nondimensionalized longitudinal coordinate of propeller position x'_P and the yaw rate r of the cargo ship.

3.2.3 Forces and moment acting on rudder

As shown in (3.10), the rudder of the ship contributes to the generation of forces and yaw moment. To determine the forces and yaw moment generated by the ship's rudder, the following calculations can be employed:

$$X_R = -(1 - t_R) F_N \sin\delta \tag{3.20a}$$

$$Y_R = -(1 + a_H) F_N \cos\delta \tag{3.20b}$$

$$N_R = -(x_R - a_H x_H) F_N \cos\delta \tag{3.20c}$$

here, the rudder normal force F_N, is considered, while the tangential force is neglected. The coefficients t_R, a_H, and x_H are used to account for the hydrodynamic interaction between the ship hull and rudder [42]. The t_R coefficient, known as the steering resistance deduction factor, quantifies the deduction in rudder resistance relative to $F_N \sin d$, where d represents the longitudinal component of F_N. It also includes the increase in propeller thrust induced by steering, resulting from the elevation of the nominal wake at the propeller position [43]. The a_H coefficient represents the factor by which the lateral force acting on the ship hull due to steering increases in comparison to the lateral component of $F_N \cos d$. Empirical observations from tank tests have shown that a_H typically ranges from 0.3 to 0.4 [40]. The x_H coefficient represents the longitudinal location at which an additional lateral force component acts, and it has been measured to be approximately -0.45 multiplied with the length of the ship L_{pp}, indicating that the force acts on the stern part of the hull. F_N can be calculated as follows:

$$F_N = \frac{\rho A_R U_R^2 f_\alpha \sin \alpha_R}{2} \tag{3.21}$$

where the resulting rudder inflow velocity U_R and the angle a_R can be mathematically expressed as following set of equations:

$$U_R = \sqrt{u_R^2 + v_R^2} \tag{3.22a}$$

$$\alpha_R \simeq \delta - (v_R/u_R) \tag{3.22b}$$

In equation (3.22), the variables u_R and v_R represent the longitudinal and lateral inflow velocity components to the rudder, respectively. These variables can be determined through the following calculations:

$$u_R = \varepsilon u(1-w_P)\sqrt{\eta\left\{1+\kappa\left(\sqrt{\frac{1+8K_T}{\pi {J_P}^2}}-1\right)\right\}^2+(1+\eta)} \tag{3.23a}$$

$$v_R = U\gamma_R\beta_R \tag{3.23b}$$

where ε which represents the ratio of wake fraction at the propeller position w_P to the wake fraction at the rudder positions w_R. Another parameter is η which denotes the ratio of the propeller diameter D_P to the rudder span H_R. Additionally, κ is an experimental constant used to express u_R, the inflow velocity at the rudder. The ship's speed U is the resultant of its longitudinal velocity u and sway velocity v, calculated

as $\sqrt{u^2+v^2}$. The variables γ_R and β_R represent the flow straightening coefficient and effective inflow angle to the rudder in maneuvering motions, respectively.

$$\varepsilon = \frac{1-w_R}{1-w_P} \tag{3.24a}$$

$$\beta_R = \beta - l'_R r' \tag{3.24b}$$

Here, l'_R is nondimensionalized the cargo ship's effective longitudinal coordinate of rudder position.

3.3 Model Validation

Before implementing and testing any controller designed, it is crucial to verify the accuracy of the model by comparing it with experimental results from previous studies. The validation process utilizes the results presented in [38] to assess the developed ship dynamics model. Specifically, the ship's attitude during starboard side turning with a constant rudder angle of $\delta = 35$ degrees is plotted, along with the *xy*-coordinates of the ship's location. To ensure a robust validation procedure, the DTC Container ship at a 1/80 model scale is selected as the physical ship for validation, as documented in [44]. This ship is commonly used for comprehensive documentation and standardized simulation parameters, facilitating the comparison and validation of results across different simulation tools and methodologies [45]. The geometric properties of the ship, hydrodynamic coefficients, and rudder parameters used in the simulations are detailed in Appendix A.

Figure 3.1 illustrates a comparison between the obtained turning circle test results and other experimental and numerical findings from published literature, specifically references [38] and [39]. The presented results are nondimensional, enabling standardized comparisons of trajectory data across multiple studies [46]. The objective of this figure is to demonstrate the accuracy of the trajectory approximation for a constant rudder angle of $\delta = 35$ degrees withconstant propeller speed $n_P = 11.89$ revolution/s. The actual ship trajectory, represented by the black line, is obtained from experimental measurements conducted on the real system. Notably, both the linear and nonlinear models developed in this study demonstrate a satisfactory level of agreement with the actual system, comparable to the CFD and system based results obtained from other study.

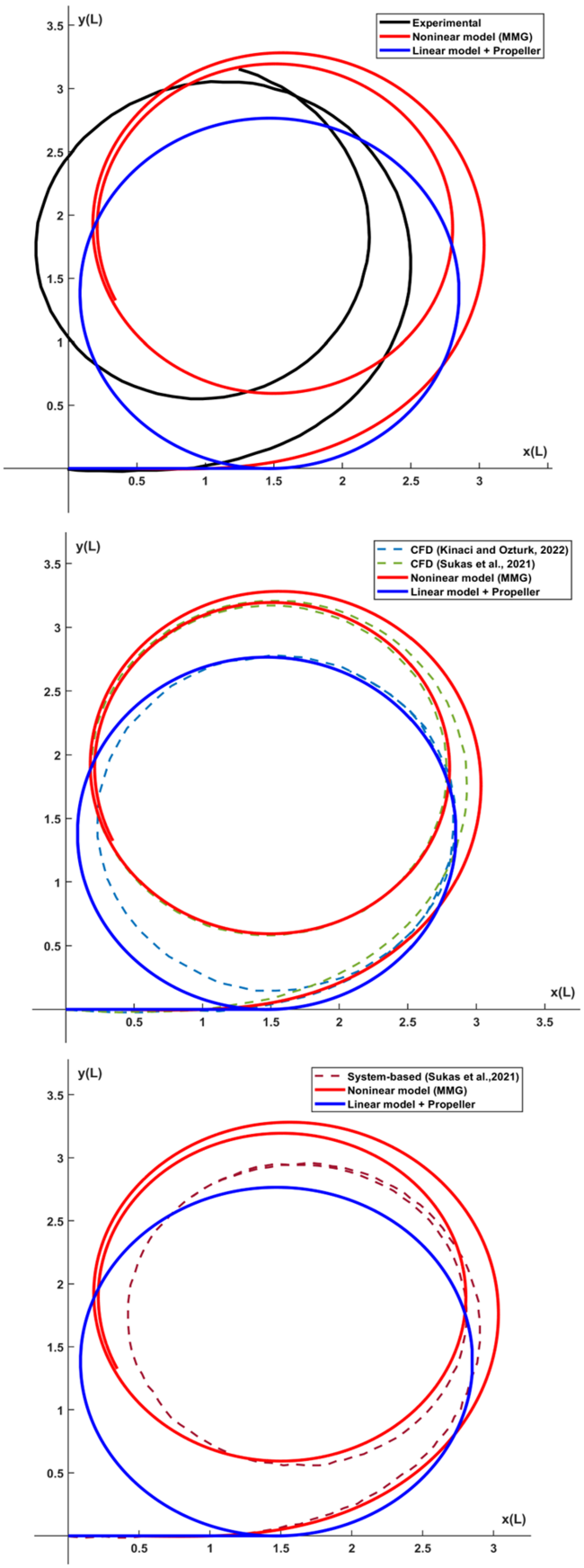

Figure 3.1 : Comparison of turning circle test results vs. Experimental (Top), vs. CFD (Middle), vs. System-based (Bottom) at a rudder angle of 35 degrees.

4. HEADING CONTROL WITH PARAMETRIC UNCERTAINTIES

Numerous studies have been conducted in the field of ship control, specifically focusing on managing uncertainties associated with hydrodynamic coefficients. Various approaches have been explored, including predictive methods like Multi-level Model Predictive Control (MPC), adaptive control techniques, fuzzy logic-based control, machine learning-based approaches such as reinforcement learning, and robust control methods.

The focus of this chapter is to implement a robust controller to address the aforementioned problem. Robust controllers utilize mathematical models that consider uncertain parameters to ensure stable and accurate ship operation under different conditions. However, finding a suitable robust controller using deterministic methods can be challenging, given the complexity of the optimization problem. The commonly used ship motion model provided by MMG, for example, has 17 coefficients for the hull's hydrodynamic coefficient alone, making the optimization problem complex and large.

4.1 Robust Syntheses to Typical Optimization Problem

Consider hydrodynamic forces acting on ship hull provided by MMG [40]:

$$X_H = \frac{\rho L_{pp} d U^2 X'_H(v'_m, r\prime)}{2} \tag{4.1a}$$

$$Y_H = \frac{\rho L_{pp} d U^2 Y'_H(v'_m, r\prime)}{2} \tag{4.1b}$$

$$N_H = \frac{\rho L_{PP}^2 d U^2 N'_H(v'_m, r\prime)}{2} \tag{4.1c}$$

X_H, Y_H and N_H are surge force, sway force and moment acting on the ship hull while prime accents denote nondimensionalized forces that can be expressed polynomial functions:

$$X'_H(v'_m, r\prime) = -R'_0 + X'_{vv}v'^2_m + X'_{vr}v'_m r\prime + X'_{rr}r'^2 + X'_{vvvv}v'^4_m \tag{4.2a}$$

$$Y'_H(v'_m, r\prime) = Y'_v v'_m + Y'_R r\prime + Y'_{vvv}v'^3_m + Y'_{vvr}v'^2_m r' + Y'_{vrr}v'_m r'^2 + Y'_{rrr}r'^3 \tag{4.2b}$$

$$N'_H(v'_m, r\prime) = N'_v v'_m + N'_R r\prime + N'_{vvv}v'^3_m + N'_{vvr}v'^2_m r' + N'_{vrr}v'_m r'^2 + N'_{rrr}r'^3 \tag{4.2c}$$

Where all of the subscripted X, Y, and N variables on the right-hand side are the hydrodynamics derivative on maneuvering which can be denoted as ϑ. With 17 parameters being considered in controlling a ship's hull, determining the optimal controller parameter through deterministic methods involves complex mathematical calculations [47]. In such cases, meta-heuristic optimization approaches such as Particle Swarm Optimization (PSO) and Genetic Algorithm (GA) are commonly used [48]. One approach to solving this problem is to define a desired cost ω_d and search for a k value that results in a cost ω less than the desired cost [49]. To accomplish this, we can frame the optimization problem as follows:

$$\omega_d \geq \omega(\vartheta, k) \tag{4.3}$$

Here, the cost ω given hydrodynamics coefficient ϑ and controller parameters k has to be less then desired cost ω_d. However, due to the fact that ϑ are generally comes with some degree of error, the optimal parameter k might not work as good as the simulated result [50]. This error generally caused by difficulties on setting up a proper experimental condition considering the nature of the sea is very dynamically uncertain [51]. Let us define parameter ϑ from experimental result as the nominal parameter ϑ_0 which is the subset of Θ which can be expressed as follows:

$$\Theta \triangleq \vartheta \in [\vartheta^-, \vartheta^+]; \vartheta^- \leq \vartheta_0 \leq \vartheta^+ \tag{4.4}$$

To be able to have a controller that can also compensate these uncertainties, controller obtained from (4.4) will not be sufficient. Instead, we need to have a robust synthesis to the equation. This can be expressed as follows:

$$\omega_d \geq \{\omega(\vartheta, k) \; \forall \; \vartheta \in \Theta\} \tag{4.5}$$

Typically, optimization problem from (4.4) solved by using meta-heuristic optimization algorithm [52] due to the complexity of the MMG model. This optimization algorithm is commonly used to find optimal solutions for complex problems

where traditional optimization methods are not effective [53]. While metaheuristic optimization such as Genetic Algorithm (GA) and Particle Swarm Optimization (PSO) have been shown to be effective at solving optimization problems without uncertainties being introduced, they can be computationally expensive, particularly when dealing with a large number of uncertain parameters. Figure 4.1 illustrates how PSO or GA would work given uncertainties problem:

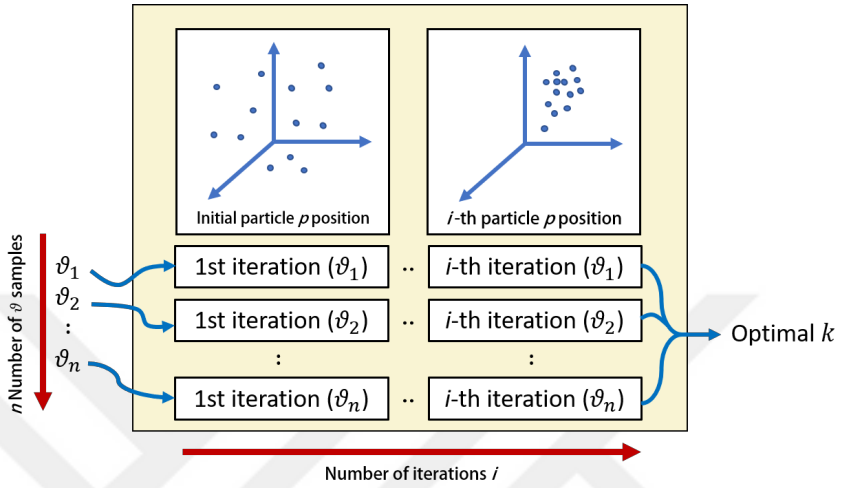

Figure 4.1 : Particle or Population Based Optimization for Multi-sample Problem.

For every sample of the model ϑ, the motion model is simulated with p number of particles for i iterations. Meaning, the number of motion model together with the control algorithm being simulated ϖ can be expressed as follow:

$$\varpi_{PSO/GA} = n.p.i_{PSO/GA} \tag{4.6}$$

As we increase the number of samples ϑ set of $[\vartheta^-, \vartheta^+]$, number of particles p, and iteration $i_{PSO/GA}$ to be dense enough in order to obtain desired accuracy [54], we significantly increase the number of models being simulated which corresponds to amount of time needed to perform the optimization process. Assume that the time taken for finding an optimal k to satisfy (4.4) is 20 hours. Then for 10,000 samples ϑ set of Θ, we are expecting 200,000 hours or approximately 25 years to solve problem from (4.5) with the same optimization algorithm. Here we learn that the existence of solution in this case is necessary but not sufficient considering the time taken to run the simulation is also an important factor. The solution of this problem requires both good result of k as well as reasonable time to run the optimization simulation.

4.2 Bisection Optimization via Blind Search

In this subchapter, an approach for optimizing the problem introduced in previous subchapter, which is the Bisection Optimization via Blind Search is presented. Unlike metaheuristic optimization solver discussed in the previous subchapter, this method works faster due to the fact it does not have the particle or population-based iteration during the optimization. The proposed method, on the other hand, does not rely with the number of particles or population. Bisection Optimization via Blind Search is a two-step optimization algorithm that utilizes a blind search technique in the first stage, followed by a refinement process using the bisection method to obtain the optimal controller. The steps involved in this method described in Figure 4.2.

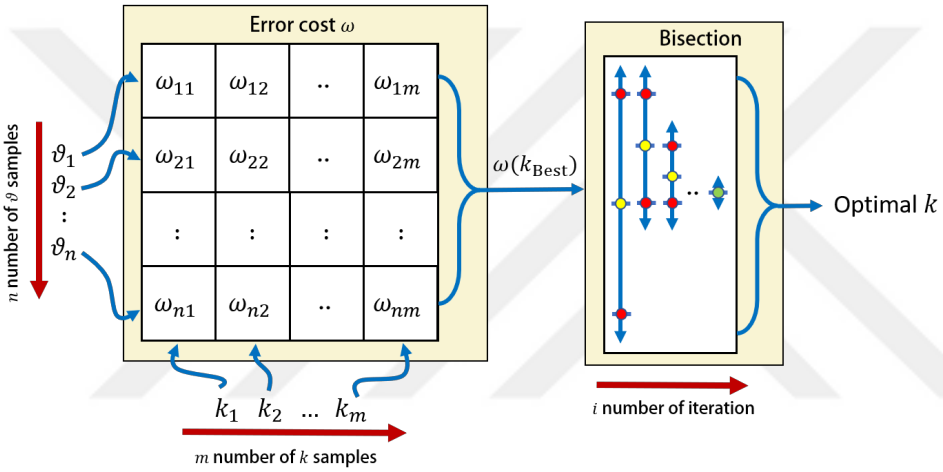

Figure 4.2 : Bisection Optimization via Blind Search for Multi-sample Problem.

In this approach, the model is simulated for n samples, using m sampled controller parameters k, and saving the resulting cost value ω. The controller parameter k, that yields the lowest value of ω is then refined in the second stage using a bisection-based optimization method. The number of simulations of the motion model and control algorithm need to be completed, denoted by ϖ, can be expressed as follows:

$$\varpi_{BB} = n(m + i_{BB}) \tag{4.7}$$

Here we can see that the number iteration of bisection method i_{BB} being added to number of k samples m compared to $i_{PSO/GA}$ which effects the number of models being simulated ϖ multiplicatively. Therefore, the algorithm being proposed can significantly reduce the optimization time needed.

4.2.1 Methods of sampling

As mentioned in the problem formulation, the hydrodynamics coefficients are the uncertain parameter in this study. A Gaussian distribution employed for random generation to account for uncertainties in the model. The reason for choosing this distribution is to treat the hydrodynamics coefficient obtained from experimental results as a valid reference for the model uncertainties. As explained previously, the uncertainty range is defined as:

$$\vartheta^{-} \leq \vartheta_0 \leq \vartheta^{+} \tag{4.8}$$

Where the mean of the distribution will be based on the nominal sample ϑ_0, while the standard deviation of the distribution will determine the level of error associated with the hydrodynamics coefficient. The distribution of model uncertainties and the impact of standard deviation on its shape are visually illustrated in Figure 4.3.

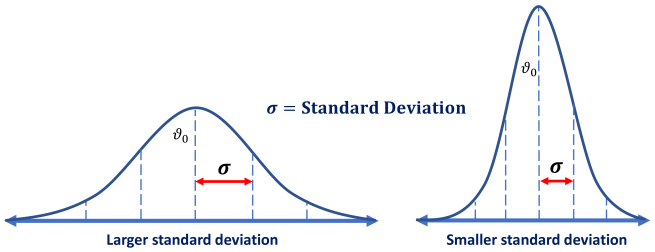

Figure 4.3 : Gaussian-based sampling of model uncertainties.

The number of samples required to obtain a reliable estimate of real-world scenarios will be determined using a function introduced by Lyonett and Toscano [55], which is expressed as follows:

$$n \geq \frac{ln(1-a)}{ln(1-b)} \tag{4.9}$$

The minimum number of samples required for a reliable estimate is denoted as n, with a and b being parameters that determine the level of confidence in the sampling method. The value of a and b ranges from 0 to 1, with a larger value of a resulting in a greater number of samples needed, and a larger value of b requiring fewer samples.

In contrast to the sampling of model uncertainties, the controller parameters k are randomly generated using a uniform distribution, as there is no prior information about the optimal controller [56]. The process involves specifying the search interval and the

required number of samples. The value of n obtained from (4.9) is used to determine the number of k samples.

4.2.2 Performance criterion

The evaluation of a controller's performance during the optimization process conducted through the use of a cost function. Four distinct types of error-based cost functions J are considered, namely: Integral of Absolute Error (IAE); Integral of Squared Error (ISE); Integral of Time multiplied Absolute Error (ITAE); and Integral of Time multiplied Squared Error (ITSE). Table 4.1 shows mathematical expressions and descriptions of all mentioned functions.

Table 4.1 : Cost functions and their respective equations.

Cost Function	Equation
IAE	$J_{IAE} = \int \|e\| dt$
ISE	$J_{ISE} = \int e^2 dt$
ITAE	$J_{ITAE} = \int t\|e\| dt$
ITSE	$J_{ITSE} = \int te^2 dt$

IAE measures the steady-state error of a control system by minimizing the integral of the absolute error over time [57, 58]. Similarly, ISE minimizes the integral of the squared error over time, making it suitable for evaluating the steady-state error of a control system [57–59]. ITAE, on the other hand, is designed to minimize the integral of the absolute error over time while prioritizing fast and accurate response times [57]. This cost function is commonly used in systems that require quick and precise responses [57, 60]. Finally, ITSE computes the integral of the absolute error over time, making it suitable for systems that require fast and accurate response times but may be more sensitive to overshoot or oscillation [56, 58, 59].

4.3 Autonomous Cargo Ship Heading Control Strategies

The domain of autonomous cargo ship heading control is a critical aspect of ensuring accurate navigation and efficient course following. With the rise of autonomous vessels, achieving precise and robust heading control has become an essential objective. This chapter provides an in-depth analysis of PID-based control

strategies employed in autonomous cargo ship heading control, with constant propeller revolution speed.

By virtue of its simplicity, versatility, and robustness, the PID-based controller emerges as an optimal choice for autonomous cargo ship heading angle control in real-time scenarios. Notably, its efficacy stems from the capacity to finely tune control parameters, ensuring desired performance characteristics encompassing stability, responsiveness, and steady-state accuracy. Leveraging the PID controller, autonomous cargo ships can attain and sustain precise heading angles, culminating in improved navigation accuracy, efficient route planning, and heightened overall operational efficiency, thereby bolstering the viability and advancement of autonomous maritime transportation.

4.3.1 P controller

The proportional (P) controller can be considered as the most elementary variant among the PID-based controller family. Figure 4.4 depicts a diagrammatic illustration outlining the operational scheme of the P controller for cargo ship's heading tracking control.

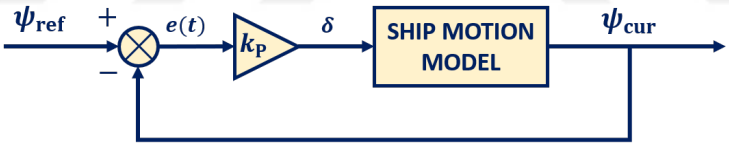

Figure 4.4 : Block Diagram of control system with P controller.

This operational scheme entails the calculation of the disparity between the reference heading angle ψ_{ref}, and the present heading angle ψ_{cur}. Subsequently, this error is multiplied by the proportional gain coefficient k_P [61]. This sequence of input signal δ calculation can be mathematically represented by the following equation:

$$\delta = k_P(\psi_{ref} - \psi_{cur}) \tag{4.10}$$

4.3.2 PD controller

The Proportional-Derivative (PD) controller surpasses the Proportional (P) controller as an optimal choice for ship heading tracking control, primarily due to its capacity to mitigate oscillations and improve overall system performance [62]. Unlike the

P controller that solely considers the current heading angle error, the PD controller incorporates both the error $e(t)$ and the rate of change of the heading angle ψ. This concise introduction highlights the superior attributes of the PD controller in ship heading control, emphasizing its ability to effectively reduce oscillations and enhance tracking precision. Figure 2 visually depicts the operational mechanism of the PD controller, further elucidating its role in ship heading tracking control.

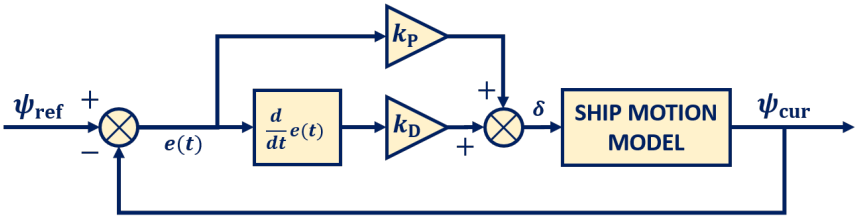

Figure 4.5 : Block Diagram of control system with PD controller.

The computation process for the PD controller in a discrete system, as depicted in Figure 4.5, can be mathematically expressed as follows:

$$\delta = k_P(\psi_{ref} - \psi_{cur}) + k_D \frac{d}{dt}(\psi_{ref} - \psi_{cur}) \tag{4.11}$$

Here the computation of the rudder angle δ in the PD controller involves the summation of two terms. The first term is obtained by multiplying k_P with the error $e(t)$. The second term is obtained by multiplying the derivative term of the controller k_D with the derivation of $e(t)$ with respect to time.

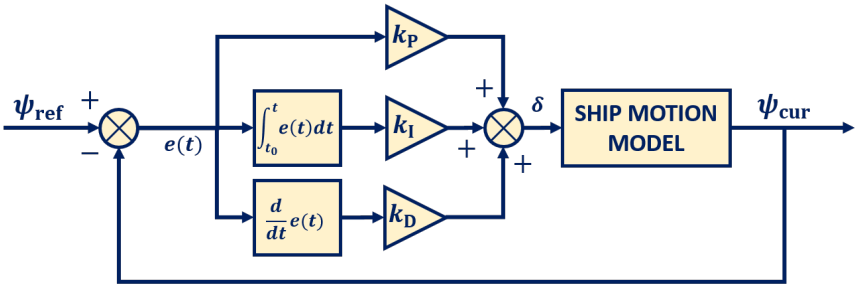

Figure 4.6 : Block Diagram of control system with PID controller.

4.3.3 PID controller

While the P or PD controller adjusts the control variable based on the current error or the error and its rate of change, respectively, the Proportional-Integral-Derivative (PID) controller incorporates an additional integral control component to address steady-state errors. By integrating the historical error over time, the PID controller improves accuracy and stability, making it a versatile and essential control algorithm in various applications [63]. Figure 4.6 illustrates the working principle of a PID controller in controlling the ship's heading angle.

The relationship between the integral term and the other components in the determination of δ is defined as follows:

$$\delta = k_P(\psi_{ref} - \psi_{cur}) + k_D \frac{d}{dt}(\psi_{ref} - \psi_{cur}) + k_I \int_{t_0}^{t} e(t)\,dt \tag{4.12}$$

where PID control introduces an additional integral term k_I in the computation of the control variable δ. This term are multiplication of k_I and the integration of $e(t)$ over time.

In this study, the consideration of a Proportional-Integral (PI) controller was omitted due to the specific requirements of ship motion control applications. While the integral term in the PID controller aims to eliminate steady-state error, it is not the primary focus in ship motion control. The main objectives in this context are efficient point-to-point movement, which can be addressed by the proportional term k_P, and ensuring comfort and safety by reducing oscillations, which can be handled by k_D. Thus, it was determined that studying the PI controller is unnecessary for ship motion applications, given the specific goals and priorities of this domain.

4.4 Optimization Parameters and Results

A simulation scenario created where the controller is given a task of changing the yaw angle ψ, from 0 degree to 40 degree. To evaluate the effectiveness of the controller, the study introduced varying levels of uncertainty to assess its ability at maintaining stability with tolerable variations in the system parameters. In this thesis, the levels of uncertainty considered to be $\pm 20\%$ which represent the extent to which the parameters can deviate from their nominal values.

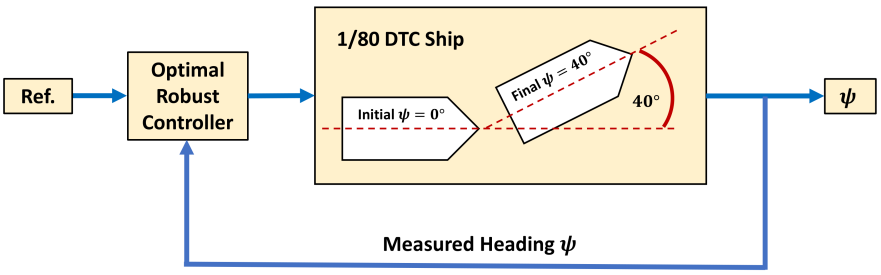

Figure 4.7 : Heading angle ψ control optimization.

Figure 4.7 illustrates the scenario for the optimization. The output Optimal Robust Controller block is rudder angle δ which has angle saturation max. 35 degree and turning rate saturation of max. 10 degrees/second. The ship has initial surge speed 1.179 m/s and the propeller speed is 5 revolutions/second.

4.4.1 Initialization of optimization process

In this study, two types of controllers were investigated, namely proportional (P) and proportional-derivative (PD) controllers. The justification of derivative term inclusion is to damp out oscillations or overshoot in the system's response which can improve the stability and settling time [53]. On the other hand, the integral term considered to be excluded due to the system's inherent stability [57] and expected slow response.

Table 4.2 : Bisection Optimization via Blind Search Properties.

Optimization Parameters	
$S_{1,BB}$	0
$S_{2,BB}$	100
d	5
m	10,000
a	0.995
b	0.005

Optimization parameters can be seen in Table 4.2 where 10,000 controller parameter k is sampled with lower search bound $S_1 = 0$ and upper interval bound $S_2 = 100$. The initial bisection interval $d = 5$ and we obtain number of uncertainties sample $n = 1058$ which determined from parameter a and b as shown in (4.9).

4.4.2 Optimization results

The simulation was run on a computer with an Intel Core i7-9750H, 20GB of RAM, an NVIDIA Quadro T1000 graphics card and the simulation software used is MATLAB R2022b. The total elapsed time for each optimization is approximately 15 hours.

Table 4.3 : Optimization Results.

Cost	P controller		PD Controller		
Function	k_P	Cost	k_P	k_D	Cost
IAE	2.70	7632.63	1.83	10.30	6684.96
ISE	2.51	3365.27	1.45	11.01	2709.62
ITAE	2.81	69776.19	1.84	10.31	47857.26
ITSE	2.62	15128.92	1.80	10.27	12229.44

Both P and PD-controller has same amount of controller parameter being sampled m. The only difference is PD controller has pairs of $k = [k_P, k_D]$, instead of only k_P. The results are listed in Table 4.3. All error criterion provides practically the same result although the decimals are varied. Cost functions which employ a time multiplicative factor (ITAE and ITSE) demonstrate a slightly larger k_P value compared to IAE and ISE. Nevertheless, the main insight from the table is it can be seen that PD-controller outperformed the P controller, as lower cost associated with the former. It should be noted that the comparison of costs between different error criterion is not meaningful, since each of them employs a different equation to calculate the error.

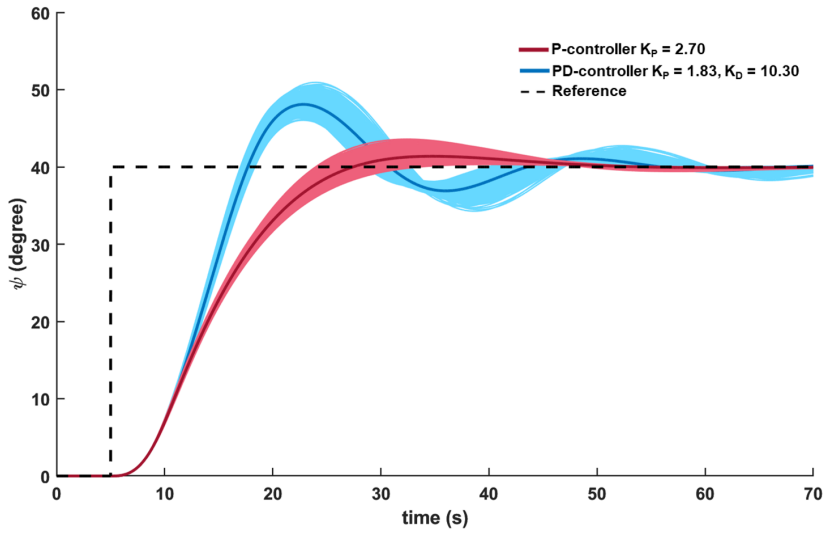

Figure 4.8 : System responses with P and PD-controller via IAE.

In order to visualize the result from Table 4.3, optimum controller obtained via IAE selected arbitrarily to be plotted in Figure 4.8. Darker lines represent the system response in the ideal condition where there are no hydrodynamic coefficients error while the lighter colored regions are actually a group of densely stacked lines that represents the system response with 1058 random gaussian variation of hydrodynamic coefficient with 20% level of uncertainty. It can be observed that adding derivative term into controller gives a damping effect on the system's response that reduce overshoot and oscillations, resulting in a faster settling time.

4.4.3 Computational Efficiency Comparison

The computational efficiency of the proposed optimization method is compared with the conventional PSO algorithm in terms of the execution time needed to achieve the optimal solution within a desired tolerance. As discussed previously, conducting PSO optimization for the entire range of sampled uncertainty variation $(n = 1058)$ is impractical. Therefore, in this simulation, the focus is only on the nominal value. The PSO optimization parameters are provided in Table 4.4.

Table 4.4 : Particle Swarm Optimization Properties.

Optimization Parameters	
$S_{1,PSO}$	0
$S_{2,PSO}$	100
N	100
Stopping Criterion	If $\delta k_P, \delta k_D \leq 0.01$
Cost Function	IAE

here, a swarm size of $N = 100$ employed and the stopping criterion selected based on the requirement of considering only 2 decimal places, as shown in Table 4.4. The simulation was conducted only for PD controller, as P controller did not yield satisfactory results in the previous section. Again, IAE arbitrarily selected for error criterion as the other three cost functions provide relatively similar results. After 7 iterations which took approximately 19 minutes, $k_P = 4.17$ and $k_D = 9.35$ obtained.

The obtained controller parameters obtained via PSO algorithm are tested in a same simulation scenario introduced previously. and the system's responses are compared in Figure 4.9. The simulation results demonstrate that in conditions of ideal situations (0%) or low uncertainty (5%), PD-controller from PSO algorithm arguably provides

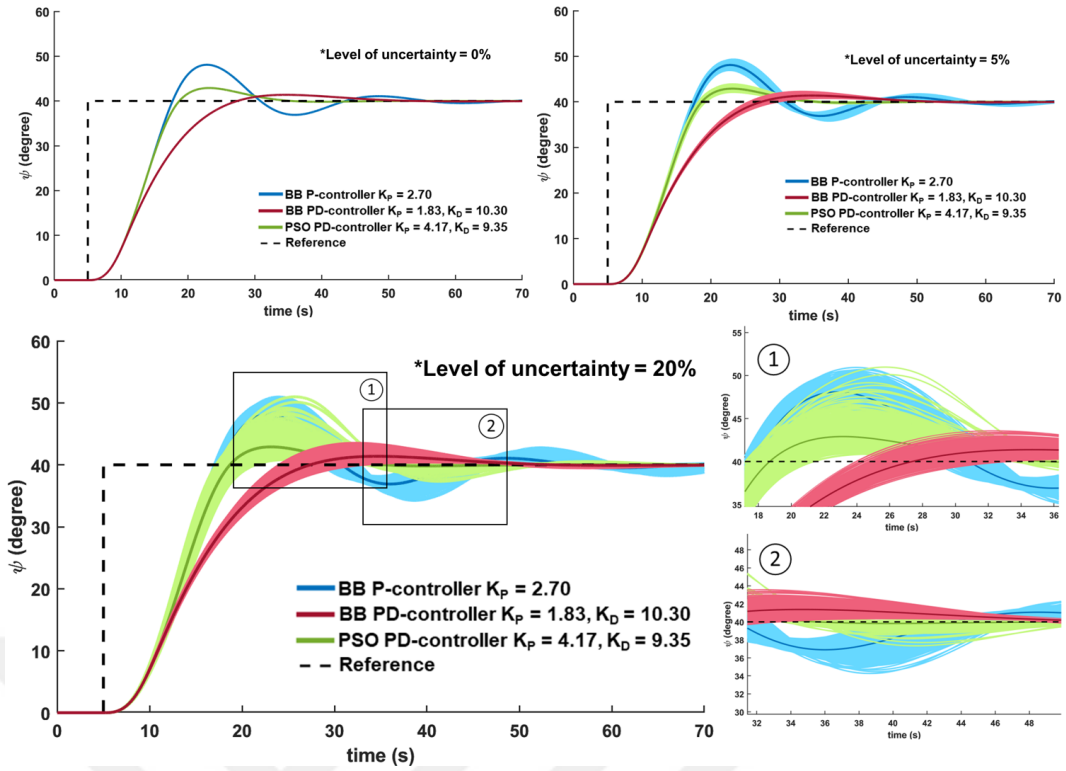

Figure 4.9 : System responses with P/PD-controller from proposed method and PD-controller from PSO for $0\%, 5\%$, and 20% level of uncertainties.

the best performance for ship motion control. Although some small overshoot is observed, the settling time is quicker compared to other methods. However, as the level of uncertainty increases to 20%, undesired behavior starts to appear. For certain combinations of parameter variations, the system response yields 25% overshoot, which is not desirable in ship motion control. In contrast, the PD-controller obtained from Bisection Optimization via Blind Search shows a more stable response and quicker overall settling time in higher uncertainty conditions. This can be attributed to the fact that the PD-controller via our proposed method considers all possible model parameter variations $(n = 1058)$ while the PSO algorithm does not. If all model samples were to be considered in PSO algorithm, the simulation time required would be approximately become 19 minutes multiplied 1058 samples which resulting the total of 22218 minutes, or around 14 days. This shows that the proposed method is 22 times faster.

4.5 Test Cases

In this section, additional tests conducted to further enhance our comprehension of how well the controllers perform. These tests involved three different scenarios: Step, M-Turn, and Doublet maneuver test. The ship provided with a set of position coordinates in the form of x and y references. The reference coordinates which used the ship's length L as a reference point are listed in Table 4.5. We varied the locations to see if the control system could handle different scenarios effectively.

Table 4.5 : x and y coordinate references.

Step		M-Turn		Doublet	
$x(L)$	$y(L)$	$x(L)$	$y(L)$	$x(L)$	$y(L)$
0	0	0	0	0	0
1	0	1	1	1	0
3	1	2	-1	1	1
3	1	3	1	2	1
–	–	4	0	2	-1
–	–	–	–	3	-1
–	–	–	–	3	0
–	–	–	–	4	0

The ship's ability to reach each point is the main objective in this test cases, rather than the specific angle at which it arrives or which path it should follow. Fig. 4.10 illustrates the control loop for these test cases, which outlines the steps involved in the process.

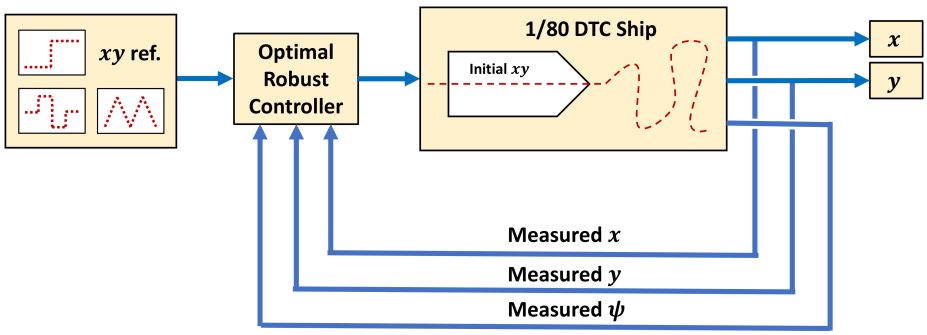

Figure 4.10 : Waypoint control of 1/80 DTC Ship.

It is apparent that the system references are given in $xy-$coordinates, whereas the input of the system requires heading angle as a reference. Hence, a transformation

is necessary to convert the input reference from $xy-$coordinates to a heading angle reference. This can be formulated as follow [64]:

$$\psi_{ref} = arctan2\left(\frac{y_{ref} - y_{meas}}{x_{ref} - x_{meas}}\right) \tag{4.13}$$

where x_{ref} and y_{ref} are x and y coordinates reference respectively while x_{meas} and y_{meas} are measured coordinates at current time step. The process of feeding input to the controller is done incrementally, one reference point at a time where the ship must be within 50 cm of the current reference point before the next reference point can be tracked.

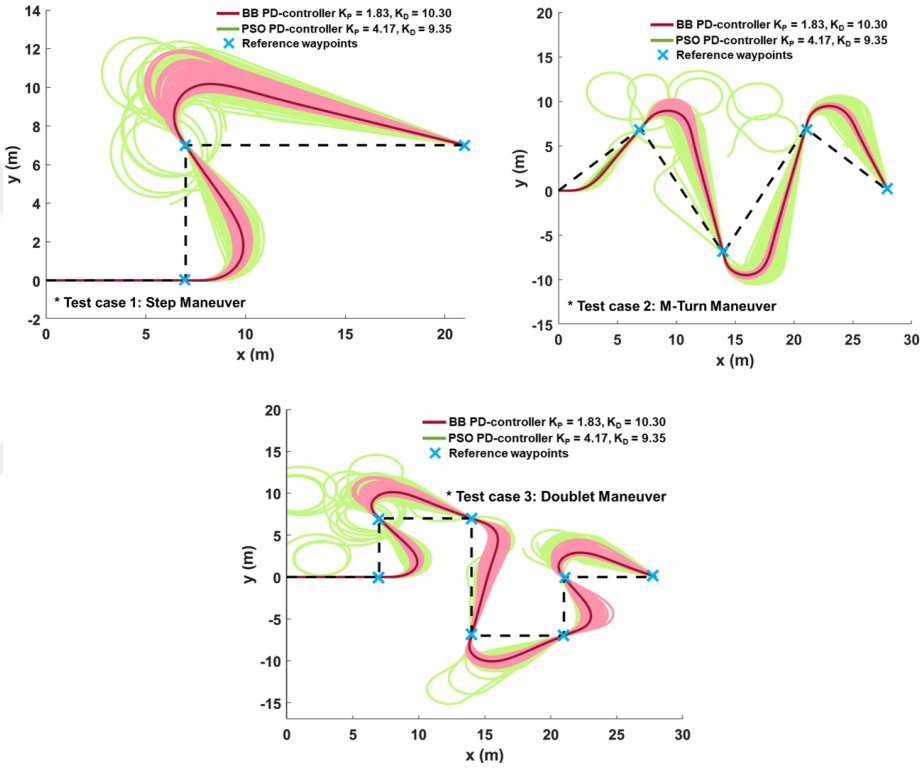

Figure 4.11 : Ship maneuver test cases for 20% uncertainty level.

Figure 4.11 compares the paths taken by a 1/80 DTC ship controlled by PD-controllers obtained using Bisection Optimization via Blind Search and the Particle Swarm Optimization algorithm. The controller obtained by our proposed method is capable of tracking all of the given reference waypoints. In contrast, the controller obtained from PSO algorithm, which is designed only for nominal parameter values, encounters difficulty when uncertainty introduced.

5. CONCLUSION

This thesis has explored control strategies and optimization approaches to effectively address the presence of parametric uncertainty in ship hydrodynamics for autonomous cargo ships. The research objective was to develop control-oriented models and methodologies that enhance the maneuverability and performance of cargo ships under uncertain hydrodynamic parameters.

Validation of the proposed approach through turning circle tests has provided promising results. Comparisons with other experimental and numerical studies have showcased the capability of the developed models, both linear and nonlinear, to approximate the actual ship trajectory. The level of agreement observed, comparable to computational fluid dynamics (CFD) results, confirms the practicality and accuracy of the proposed control strategies and optimization approaches.

The control strategies developed in this research have focused on proportional-derivative (PD) control methods. Considering the nature of ship dynamics and the desired objectives, it was determined that integral control parameters do not play a significant role in ship control. The emphasis was placed on reducing steady-state error and minimizing oscillatory motions for improved comfort and stability. Therefore, the PD control approach was deemed suitable for achieving the desired ship control performance.

To address the parametric uncertainty, a novel optimization technique called "Bisection Method via Blind Search" was proposed. This technique aims to optimize the control inputs in the presence of uncertain parameters, effectively improving the robustness and adaptability of the control system. By systematically exploring the parameter space through a blind search approach, the optimization process can converge to a suitable control solution that mitigates the impact of parametric uncertainty on ship hydrodynamics.

The implications of this research extend to the field of autonomous shipping, where precise and reliable ship control is essential. The developed control strategy, based on PD control, offers a practical and efficient approach for autonomous cargo ships to navigate, maneuver, and maintain desired trajectories. The integration of the proposed optimization technique further enhances the adaptability and robustness of the control system, ensuring safe and efficient operations in diverse maritime environments.

In acknowledging the limitations of this study, it is important to note that the control strategies developed in this research do not explicitly consider disturbances during the control phase, such as wave and wind disturbances. These external factors can significantly impact the performance and stability of autonomous cargo ships. Therefore, a potential avenue for future work would be to incorporate control-oriented wave and wind disturbance models to enhance the effectiveness of the proposed control strategies presented in this thesis. By accounting for these disturbances, the control system can be further optimized to ensure robust and reliable ship control under varying environmental conditions. Addressing the influence of disturbances will contribute to a more comprehensive and realistic control framework for autonomous cargo ships, enhancing their operational capabilities in real-world scenarios.

Looking ahead, future research opportunities lie in the exploration of advanced control algorithms, such as model predictive control (MPC), adaptive control, or fuzzy logic control, to further improve the ship's maneuverability and response in dynamic conditions. Additionally, the optimization techniques can be expanded to consider more complex uncertainties and constraints, allowing for even more optimized ship control strategies.

In conclusion, this thesis has successfully developed and evaluated control strategies for addressing parametric uncertainty in ship hydrodynamics. The utilization of PD control and the proposed "Bisection Method via Blind Search" optimization technique has demonstrated their effectiveness in achieving precise and stable ship control. The research outcomes contribute to the advancement of autonomous cargo ship control, paving the way for safe, efficient, and reliable autonomous shipping operations.

REFERENCES

[1] **Wang, W. and Liu, C.** (2021). An efficient ship autopilot design using observer-based model predictive control, *Proceedings of the Institution of Mechanical Engineers, Part M: Journal of Engineering for the Maritime Environment*, *235*(1), 203–212.

[2] **Ghaemi, R.**, **Oh, S. and Sun, J.** (2010). Path following of a model ship using model predictive control with experimental verification, *Proc. American Control Conference*, IEEE, pp.5236–5241.

[3] **Zhang, G.**, **Zhang, X. and Zheng, Y.** (2015). Adaptive neural path-following control for underactuated ships in fields of marine practice, *Ocean Engineering*, *104*, 558–567.

[4] **Ahmed, Y.A. and Hasegawa, K.** (2016). Fuzzy reasoned waypoint controller for automatic ship guidance, *IFAC-PapersOnLine*, *49*(23), 604–609.

[5] **Sandler, M.**, **Wahl, A.**, **Zimmermann, R.**, **Faul, M.**, **Kabatek, U. and Gilles, E.D.** (1996). Autonomous guidance of ships on waterways, *Robotics and Autonomous Systems*, *18*(3), 327–335.

[6] **Perera, L.P.**, **Carvalho, J.P. and Soares, C.G.** (2009). Autonomous guidance and navigation based on the COLREGs rules and regulations of collision avoidance, *Proc. International Workshop Advanced Ship Design for Pollution Prevention*, pp.205–216.

[7] **Reyhanoglu, M.** (1997). Exponential stabilization of an underactuated autonomous surface vessel, *Automatica*, *33*(12), 2249–2254.

[8] **Caccia, M.**, **Bibuli, M.**, **Bono, R. and Bruzzone, G.** (2008). Basic navigation, guidance and control of an unmanned surface vehicle, *Autonomous Robots*, *25*(4), 349–365.

[9] **Sonnenburg, C.R. and Woolsey, C.A.** (2013). Modeling, identification, and control of an unmanned surface vehicle, *Journal of Field Robotics*, *30*(3), 371–398.

[10] **Haseltalab, A.**, **Negenborn, R.R. and Lodewijks, G.** (2016). Multi-level predictive control for energy management of hybrid ships in the presence of uncertainty and environmental disturbances, *IFAC-PapersOnLine*, *49*(3), 90–95.

[11] **Lu, X.**, **Liu, Z. and Chu, Z.** (2020). Nonlinear adaptive heading control for an underactuated surface vessel with constrained input and sideslip angle compensation, *Brodogradnja: Teorija i praksa brodogradnje i pomorske tehnike*, *71*(3), 71–87.

[12] **Chen, X. and Tan, W.W.** (2013). Tracking control of surface vessels via fault-tolerant adaptive backstepping interval type-2 fuzzy control, *Ocean Engineering*, *70*, 97–109.

[13] **Zhang, Y.**, **Wu, C.**, **Qiao, C.**, **Sadek, A. and Hulme, K.F.** (2022). A cognitive computational model of driver warning response performance in connected vehicle systems, *IEEE Transactions on Intelligent Transportation Systems*, *23*(9), 14790–14805.

[14] **Ye, J.**, **Roy, S.**, **Godjevac, M. and Baldi, S.** (2019). Observer-based robust control for dynamic positioning of large-scale heavy lift vessels, *IFAC-PapersOnLine*, *52*(3), 138–143.

[15] **Zhang, M.**, **Taimuri, G.**, **Zhang, J. and Hirdaris, S.** (2023). A deep learning method for the prediction of 6-DoF ship motions in real conditions, *Proceedings of the Institution of Mechanical Engineers, Part M: Journal of Engineering for the Maritime Environment*, 14750902231157852.

[16] **Yasukawa, H.**, **Hasnan, M. and Matsuda, A.** (2021). Validation of 6-DOF motion simulations for ship turning in regular waves, *Journal of Marine Science and Technology*, 1–16.

[17] **Ren, Z.**, **Han, X.**, **Yu, X.**, **Skjetne, R.**, **Leira, B.J.**, **Sævik, S. and Zhu, M.** (2023). Data-driven simultaneous identification of the 6DOF dynamic model and wave load for a ship in waves, *Mechanical Systems and Signal Processing*, *184*, 109422.

[18] **Zhou, B.**, **Qi, X.**, **Zhang, J. and Zhang, H.** (2021). Effect of 6-DOF Oscillation of Ship Target on SAR Imaging, *Remote Sensing*, *13*(9), 1821.

[19] **Martelli, M.**, **Viviani, M.**, **Altosole, M.**, **Figari, M. and Vignolo, S.** (2014). Numerical modelling of propulsion, control and ship motions in 6 degrees of freedom, *Proceedings of the Institution of Mechanical Engineers, Part M: Journal of Engineering for the Maritime Environment*, *228*(4), 373–397.

[20] **Tang, G.**, **Lei, J.**, **Li, F.**, **Zhu, W.**, **Xu, X.**, **Yao, B.**, **Claramunt, C. and Hu, X.** (2023). A modified 6-DOF hybrid serial–parallel platform for ship wave compensation, *Ocean Engineering*, *280*, 114336.

[21] **Liu, L.**, **Yang, Y. and Peng, T.** (2022). Machine learning prediction of 6-DOF motions of KVLCC2 ship based on RC model, *Journal of Ocean Engineering and Science*.

[22] **Lab., D.**, `https://www.stevens.edu/davidson-laboratory`, alındığı tarih: 24.05.2023.

[23] **Gertler, M.** (1966). COOPERATIVE ROTATING-ARM AND STRAIGHT-LINE EXPERIMENTS WITH ITTC STANDARD MODEL (MARINER TYPE SHIP)., **Technical Report**, DAVID TAYLOR MODEL BASIN WASHINGTON DC HYDROMECHANICS LAB.

[24] **Shenoi, R.R.**, **Krishnankutty, P.**, **Selvam, R.P. and Kulsreshtha, A.** (2013). Prediction of maneuvering coefficients of a container ship by numerically simulating HPMM using RANSE based solver, *3rd International Conference on Ship Manoeuvring in Shallow and Confined Water, Ghent, Belgium*.

[25] **Centre, K.S.R.**, `https://krylov-centre.ru/en/experimental/basin-circle/`, alındığı tarih: 24.05.2023.

[26] **Eda, H.**, **Falls, R. and Walden, D.A.** (1979). Ship maneuvering safety studies, **Technical Report**.

[27] **Feldman, J.** (1987). Straightline and rotating arm captive-model experiments to investigate the stability and control characteristics of submarines and other submerged vehicles, **Technical Report**, David Taylor Research Center Bethesda MD Ship Hydromechanics Dept.

[28] **Derradji, A. and Van, T.** (2004). Terry fox resistance tests–Phase III (PMM) ITTC experimental uncertainty analysis iniative, **Technical Report**, Report No. TR-2004.

[29] **Kim, H.**, **Akimoto, H. and Islam, H.** (2015). Estimation of the hydrodynamic derivatives by RaNS simulation of planar motion mechanism test, *Ocean engineering*, *108*, 129–139.

[30] **Comstock, E.N. and Keane Jr, R.G.** (1980). Seakeeping by design, *Naval Engineers Journal*, *92*(2), 157–178.

[31] **Kim, D.J.**, **Kim, S.Y.**, **You, Y.J.**, **Rhee, K.P.**, **Kim, S.H. and Kim, Y.G.** (2013). Design of high-speed planing hulls for the improvement of resistance and seakeeping performance, *International Journal of Naval Architecture and Ocean Engineering*, *5*(1), 161–177.

[32] **Luhulima, R.B.**, **Setyawan, D.**, **Utama, I. and Utama, A.** (2014). Selecting monohull, catamaran and trimaran as suitable passenger vessels based on stability and seakeeping criteria, *The 14th International Ship Stability Workshop (ISSW)*, volume 29, pp.262–266.

[33] **Aertssen, G. and Van Sluys, M.** (1972). Service performance and seakeeping trials on a large containership, *Royal Institution of Naval Architects Transactions*, *114*.

[34] **Bittner, A.C.** (1985). Human factors engineering principles for minimizing adverse ship motion effects: Theory and practice, *Naval Engineers Journal*, *97*(4), 205–213.

[35] **Tzeng, C.Y. and Chen, J.F.** (2009). Fundamental properties of linear ship steering dynamic models, *Journal of Marine Science and Technology*, *7*(2), 2.

[36] **Matusiak, J.** *et al.* (2017). *Dynamics of a rigid ship*, Aalto University.

[37] **Kinaci, O.K.**, **Gokce, M.K.**, **Alkan, A.D. and Kukner, A.** (2018). On self-propulsion assessment of marine vehicles, *Brodogradnja: Teorija i praksa brodogradnje i pomorske tehnike*, *69*(4), 29–51.

[38] **Kinaci, O.K. and Ozturk, D.** (2022). Straight-ahead self-propulsion and turning maneuvers of DTC container ship with direct CFD simulations, *Ocean Engineering*, *244*, 110381.

[39] **Sukas, O.F.**, **Kinaci, O.K. and Bal, S.** (2021). Asymmetric ship maneuvering due to twisted rudder using system-based and direct CFD approaches, *Applied Ocean Research*, *108*, 102529.

[40] **Yasukawa, H. and Yoshimura, Y.** (2015). Introduction of MMG standard method for ship maneuvering predictions, *Journal of Marine Science and Technology*, *20*, 37–52.

[41] **Newman, J.N.** (2018). *Marine hydrodynamics*, The MIT press.

[42] **Bertram, V.** (2011). *Practical ship hydrodynamics*, Elsevier.

[43] **Nakos, D. and Sclavounos, P.** (1991). Ship motions by a three-dimensional Rankine panel method.

[44] **Sprenger, F.**, **Hassani, V.**, **Maron, A.**, **Delefortrie, G.**, **Van Zwijnsvoorde, T.**, **Cura-Hochbaum, A. and Lengwinat, A.** (2016). Establishment of a validation and benchmark database for the assessment of ship operation in adverse conditions, *Proc. ASME International Conference on Offshore Mechanics and Arctic Engineering*, volume49927, p.V001T01A039.

[45] **Liu, C.**, **Wang, J. and Wan, D.** (2018). CFD computation of wave forces and motions of DTC ship in oblique waves, *International Journal of Offshore and Polar Engineering*, *28*(02), 154–163.

[46] **Feng, D.**, **Ye, B.**, **Zhang, Z. and Wang, X.** (2020). Numerical simulation of the ship resistance of KCS in different water depths for model-scale and full-scale, *Journal of Marine Science and Engineering*, *8*(10), 745.

[47] **Lu, S.**, **Wang, C.**, **Fan, Y. and Lin, B.** (2021). Robustness of building energy optimization with uncertainties using deterministic and stochastic methods: Analysis of two forms, *Building and Environment*, *205*, 108185.

[48] **Sabet, M.**, **Fathi, A. and Daniali, H.M.** (2016). Optimal design of the Own Ship maneuver in the bearing-only target motion analysis problem using a heuristically supervised Extended Kalman Filter, *Ocean Engineering*, *123*, 146–153.

[49] **Emilia, F. and Uri, S.** (2005). Stability and guaranteed cost control of uncertain discrete delay systems [J], *International Journal of Control*, *78*(4), 235–246.

[50] **Keel, L. and Bhattacharyya, S.** (1994). Control system design for parametric uncertainty, *International Journal of Robust and Nonlinear Control*, *4*(1), 87–100.

[51] **Dai, K. and Li, Y.** (2021). Experimental and numerical investigation on maneuvering performance of small waterplane area twin hull, *Brodogradnja: Teorija i praksa brodogradnje i pomorske tehnike*, *72*(2), 93–114.

[52] **Koumboulis, F.N. and Tzamtzi, M.P.** (2007). A metaheuristic approach for controller design of multivariable processes, *2007 IEEE Conference on Emerging Technologies and Factory Automation (EFTA 2007)*, IEEE, pp.1429–1432.

[53] **Joseph, S.B.**, **Dada, E.G.**, **Abidemi, A.**, **Oyewola, D.O. and Khammas, B.M.** (2022). Metaheuristic algorithms for PID controller parameters tuning: Review, approaches and open problems, *Heliyon*, e09399.

[54] **Matusuu, R. and Pekar, L.** (2017). Robust stability of thermal control systems with uncertain parameters: The graphical analysis examples, *Applied Thermal Engineering*, *125*, 1157–1163.

[55] **Toscano, R. and Lyonnet, P.** (2007). Design of a robust static output feedback controller in the case of multiple parametric uncertainties, *Transactions of the Institute of Measurement and Control*, *29*(1), 71–85.

[56] **Khargonekar, P. and Tikku, A.** (1996). Randomized algorithms for robust control analysis and synthesis have polynomial complexity, *Proceedings of 35th IEEE Conference on Decision and Control*, volume 3, IEEE, pp.3470–3475.

[57] **Dhanasekaran, B.**, **Kaliannan, J.**, **Baskaran, A.**, **Dey, N. and Tavares, J.M.R.** (2023). Load Frequency Control Assessment of a PSO-PID Controller for a Standalone Multi-Source Power System, *Technologies*, *11*(1), 22.

[58] **Mahfoud, S.**, **Derouich, A.**, **El Ouanjli, N.**, **Mossa, M.A.**, **Motahhir, S.**, **El Mahfoud, M. and Al-Sumaiti, A.S.** (2022). Comparative Study between Cost Functions of Genetic Algorithm Used in Direct Torque Control of a Doubly Fed Induction Motor, *Applied Sciences*, *12*(17), 8717.

[59] **Carrasco, D.S. and Salgado, M.E.** (2010). Optimal multivariable controller design using an ITSE performance index, *International journal of control*, *83*(11), 2340–2353.

[60] **Agrawal, A.** (2022). Analytical Study of Intelligent controller with different objective function to control a complex non-linear system, *2022 13th International Conference on Computing Communication and Networking Technologies (ICCCNT)*, IEEE, pp.1–7.

[61] **Page, P.R.**, **Abu-Mahfouz, A.M. and Yoyo, S.** (2016). Real-time adjustment of pressure to demand in water distribution systems: Parameter-less P-controller algorithm, *Procedia Engineering*, *154*, 391–397.

[62] **Tomei, P.** (1991). A simple PD controller for robots with elastic joints, *IEEE Transactions on automatic control*, *36*(10), 1208–1213.

[63] **Bennett, S.** (1993). Development of the PID controller, *IEEE Control Systems Magazine*, *13*(6), 58–62.

[64] **Xinyu, L.**, **Renxiang, B.**, **Jiaming, Y.**, **Liangqi, L. and Liyuan, S.** (2020). Nonlinear modified sliding mode control of ship heading, *2020 7th International Conference on Information Science and Control Engineering (ICISCE)*, IEEE, pp.1976–1980.

APPENDICES

APPENDIX A : Properties of 1/80 DTC Ship

APPENDIX A

Table A.1 : 1/80 DTC Ship Geometric Properties.

Geometric Properties	
L	7
m	3.27
I_z	0.2044
x_G	0.011

Table A.2 : 1/80 DTC Hull Hydrodynamics Coefficients.

Hull Hydrodynamics Coefficients					
R_0	-0.033	Y_v	-0.3579	N_v	-0.0698
X_{vv}	-0.0491	Y_r	0.127	N_r	-0.0435
X_{vr}	-0.1201	Y_{vvv}	-0.2509	N_{vvv}	-0.0588
X_{rr}	-0.0509	Y_{vvr}	0.1352	N_{vvr}	-0.0367
X_{vvv}	0	Y_{vrr}	0	N_{vrr}	-0.0367
–	–	Y_{rrr}	0	N_{rrr}	-0.0367

Table A.3 : 1/80 DTC Propeller Hydrodynamic Coefficients.

Propeller Hydrodynamic Coefficients			
k_0	-0.1060	w_{P0}	0.35
k_1	-0.3246	C_1	0
k_2	0.4594	$C_2(\beta > 0)$	1.6
t_P	0.22	$C_2(\beta < 0)$	1.1
D_P	2.6	–	–

Table A.4 : 1/80 DTC Rudder Hydrodynamic Coefficients.

Rudder Hydrodynamic Coefficients			
t_R	0	a_H	0.312
x_R	-16	a_R	-0.0655
f_α	2.747	$\gamma_R(\beta > 0)$	0.640
u_R	0.5	$\gamma_R(\beta < 0)$	0.395

CURRICULUM VITAE

Name Surname : Ahmad Irham Jambak

EDUCATION :

- **B.Eng.** : 2016, Universitas Sriwijaya, Faculty of Engineering, Department of Mechanical Engineering

PROFESSIONAL EXPERIENCE AND REWARDS:

- 2021 - 2023 Awardee of Türkiye Bursları, YTB

PUBLICATIONS, PRESENTATIONS AND PATENTS ON THE THESIS:

- **Jambak, A. I.** , Bayezit I., Kinaci, O. K., Fidan B. 2023. Control-Oriented Modeling and Cascade Control of Container Ships, *International Conference on Information, Communication and Automation Technologies*, June 11–14, Sarajevo, Bosnia and Herzegovina. pp 1-6.

- **Jambak, A. I.** , Bayezit I. 2023. Robust Optimal Control of a Nonlinear Surface Vessel Model with Parametric Uncertainties, *Brodogradnja*. vol.74, no. 3, pp. 131-143.